2015

Biomechanics of Developmental Dysplasia of the Hip - An engineering study of closed reduction utilizing the Pavlik harness for a range of subtle to severe dislocations in infants.

Victor Huayamave
University of Central Florida

BIOMECHANICS OF DEVELOPMENTAL DYSPLASIA OF THE HIP – AN ENGINEERING STUDY OF CLOSED REDUCTION UTILIZING THE PAVLIK HARNESS FOR A RANGE OF SUBTLE TO SEVERE DISLOCATIONS IN INFANTS

by

VICTOR A. HUAYAMAVE
B.S. University of Central Florida, 2008
M.S. University of Central Florida, 2010

A dissertation submitted in partial fulfillment of the requirements
for the degree of Doctor of Philosophy
in the Department of Mechanical and Aerospace Engineering
in the College of Engineering and Computer Science
at the University of Central Florida
Orlando, Florida

Spring Term
2015

Major Professor: Alain J. Kassab

ABSTRACT

Developmental Dysplasia of the Hip (DDH) is an abnormal condition where hip joint dislocation, misalignment, or instability is present in infants. Rates of incidence of DDH in newborn infants have been reported to vary between 1 and 20 per 1000 births, making it the most common congenital malformation of the musculoskeletal system. DDH early detection and treatment is critical to avoid the use of surgical treatment in infants and to prevent future complications such as osteoarthritis in adult life. To this day several non-surgical treatments involving the use of harnesses and braces have been proposed to treat DDH in infants, with the Pavlik harness being the current non-surgical standard used to treat DDH at early stages. Although the Pavlik harness has been proven to be successful treating subtle dislocations, severe dislocations do not always reduce. Until now the use of the harness remains an empirical method, and its effectiveness often depends on physician expertise or trial-error procedures; thus a clear guideline has not been established to determine the best optimal harness configuration to treat both subtle and severe dislocations. The goal of this dissertation is to understand the connection between reductions for subtle and severe dislocations and passive muscle forces and moments generated while the harness is used during treatment.

While the understanding of DDH biomechanics will provide a valuable clinically applicable approach to optimize and increase harness success rate, it is not without its difficulties. This research has created and developed a three-dimensional based on patient-specific geometry of an infant lower limb. The kinematics and dynamics of the lower limb were defined by modeling the hip, femur, tibia, fibula, ankle, foot, and toe bones. The lines of action of five (5) adductor muscles, namely, the Adductor Brevis, Adductor Longus, Adductor Magnus, Pectineus, and

Gracilis were identified as mediators of reduction and its mechanical behavior was characterized using a passive response. Four grades (1-4) of dislocation as specified by the International Hip Dysplasia Institute (IHDI) were considered, and the computer model was computationally manipulated to represent physiological dislocations. To account for proper harness modeling, the femur was restrained to move in an envelope consistent with its constraints.

The model of the infant lower limb has been used to analyze subtle and severe dislocations. Results are consistent with previous studies based on a simplified anatomically-consistent synthetic model and clinical reports of very low success of the Pavlik harness for severe dislocations. Furthermore the findings on this work suggest that for severe dislocations, the use of the harness could be optimized to achieve hyperflexion of the lower limb leading to successful reduction for cases where the harness fails.

This approach provides three main advantages and innovations: 1) the used of patient-specific geometry to elucidate the biomechanics of DDH; 2) the ability to computationally dislocate the model to represent dislocation severity; and 3) the quantification of external forces needed to accomplish reduction for severe dislocations. This study aims to offer a practical solution to effective treatment that draws from engineering expertise and modeling capabilities and also draws upon medical input. The findings of this work will lay the foundation for future optimization of non-surgical methods critical for the treatment of DDH.

To my family whose unconditional love and support always motivate me to set higher targets. This work could have not been possible without your continuous encouragement. To Alina for her patience, encouragement, and support provided throughout the dissertation process. Little Emma Victoria, I promise to make up for all the weekends I could not spent with you while I was working on my dissertation. Last but not least, to all my friends who inspired and encouraged me along the way.

ACKNOWLEDGMENTS

Special thanks to:

Professor Alain Kassab for supporting me throughout my journey towards a Ph.D. degree and sharing his enthusiasm in the exciting field of biomechanics inspiring my love of research. The academic opportunities, professional opportunities, and mentorship provided by Dr. Kassab will certainly have a major impact in my future endeavors and I am anxiously looking forward to apply everything I learned during these years at while working with the Computational Mechanics Lab in my professional career. I will forever be thankful for your advice.

Professor Eduardo Divo for introducing me to numerical research early in my undergraduate career. Dr. Divo's technical guidance has enabled me to successfully pursue an academic and research career. Additionally, I will be forever grateful to him for sharing his business vision and expertise. His professionalism and friendship will continue to influence my work in years to come.

Dr. Charles Price and the International Hip Dysplasia Institute for providing the inspiration and supporting our work at national and international conferences. I will always remember our Italy research trip since it gave us the opportunity to come face to face with the history of physicians who were the pioneers in the area of developmental dysplasia of the hip.

Professors Seetha Raghavan and Faissal Moslehy for serving on my committee and advising the work I developed on this dissertation.

All the students part of the Development Dysplasia of the Hip group at the University of Central Florida. As a group we have accomplished great milestones and the work I am presenting here would have not been possible without your input.

TABLE OF CONTENTS

LIST OF FIGURES

LIST OF TABLES

CHAPTER 1: INTRODUCTION

Using a computational approach, the work developed in this dissertation investigates the mechanical effects of developmental dysplasia of the hip in infants, which typically manifests as a misalignment of the hip joint. To this end, a patient-specific anatomical model has been created to unravel the biomechanics of developmental dysplasia of the hip. Simulation-based computational research using patient-specific anatomy has proven to be a powerful tool in the field of biomedical engineering. It has been suggested that by using such state of the art methods physicians could avoid surgery. This can account for a 70% reduction in blood stream infections. Additionally, using simulation training intervention provides a 7:1 rate of return [1]. Moreover, translational research has shown that using simulation-based techniques in obstetric simulation accounts for a 40% reduction in malpractice cases [2]. Thus, using such methods will improve decision-making to diagnose and provide customized treatment.

1.1 State of the Art Problem

At earlier stages of infant development, the hip joint is susceptible to displacements. Subtle and severe dislocations are usually detected by careful clinical examination. Identification of the condition and treatment during the neonatal period is advised to prevent the progression of subluxation into severe dislocations. Ultimately, early treatment enables proper growth of the hip joint to reduce incidences of dysplasia. Going undetected or without treatment, developmental dysplasia of the hip could progress to deformation, lost function, and eventual osteoarthritis [3].

Screening is often controversial, and in order to clearly define our problem, is necessary to understand the pathophysiology of developmental dysplasia of the hip. Classical assessment

methods of developmental dysplasia of the hip treatment include physical, radiological imaging, and ultrasound techniques.

Early treatment is always needed to avoid surgery in newborns and infants, since invasive surgery complications resulting from hip reduction might lead to femoral head osteonecrosis and redislocation. In infants up to six months of age, the Pavlik harness is the standard and preferred orthopaedic device utilized worldwide to non-surgically correct developmental dysplasia of the hip in infants. Long-term studies have shown the Pavlik harness has a 95% success ratio for subtle dysplasia and subluxations, while for severe dislocations, this success ratio reduces drastically. The harness' effectiveness often depends on physician expertise and trial-error procedures. Currently no study has yet been carried out to characterize and quantify the mechanics of developmental dysplasia of the hip utilizing the Pavlik harness to understand its failure under severe dislocations. Accepting the published rate of long-term disability caused by unsuccessful treatment of developmental dysplasia of the hip with passive corrective devices such as the Pavlik harness, and the lack of factual, concise guidelines regulating their use and construction, along with no assertive methods or procedure to determine whether successful treatment will result, other than mere chance, this dissertation will use engineering fundamentals to determine the mechanics governing the operation of the Pavlik harness in order to bring to light conclusive determinants to its mechanism of action to devise case-specific methods to actively vector the femoral head to its proper concentric position in the acetabulum, thereby decreasing the incidence of disability at cause of unsuccessful treatment of development dysplasia of the hip.

At present, there are no quantitative tools to evaluate muscle forces and moments developed in hip dislocations. Therefore, computer models can assist in developing a framework

to understand the biomechanical response of developmental dysplasia of the hip. This computer model will be able to simulate the complex interaction between muscles and bones. Furthermore, results of this study could be applied in a clinical setting and serve as an effective approach to optimize the use of the Pavlik harness.

1.2 Hip Joint Motion and Hip Dislocations

The purpose of this brief section is to provide the reader with a visual aid of anatomical terms that will be used on this dissertation. Figure 1-1 shows different grades of developmental dysplasia of the hip, where (a) represents a normal hip where the labrum envelops the head and deepens the acetabulum, (b) represents a subluxated hip where the head lies eccentrically in the acetabulum deforming it, and (c) represents a dislocated hip where the cartilaginous acetabular margin deforms and the labrum may invert and obstruct reduction [4].

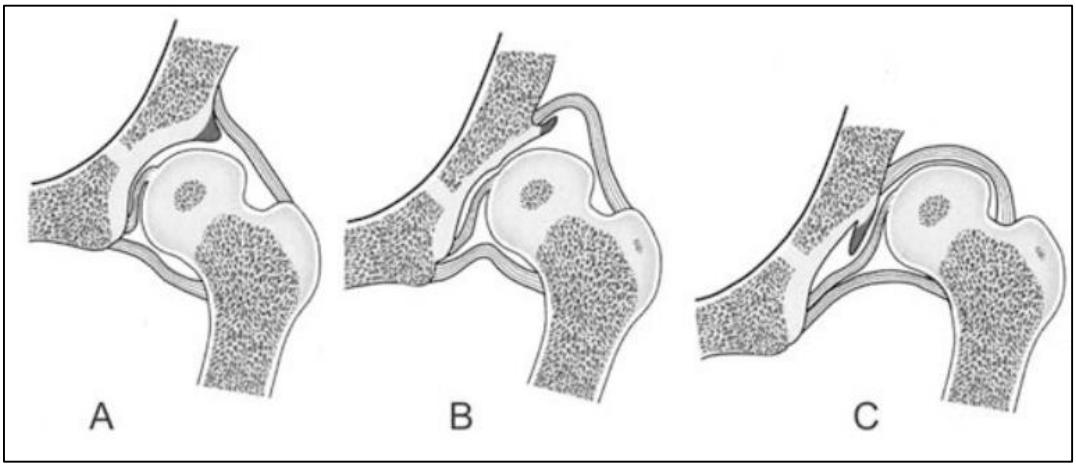

Figure 1-1:Anatomical Dislocation Classification (a) Normal Hip, (b) Subluxated Hip, and (c) Dislocated Hip [4]

Figure 1-2 exhibits hip joint and knee motion terminology that will be used on this dissertation to define functionality and ranges of motion of the joints.

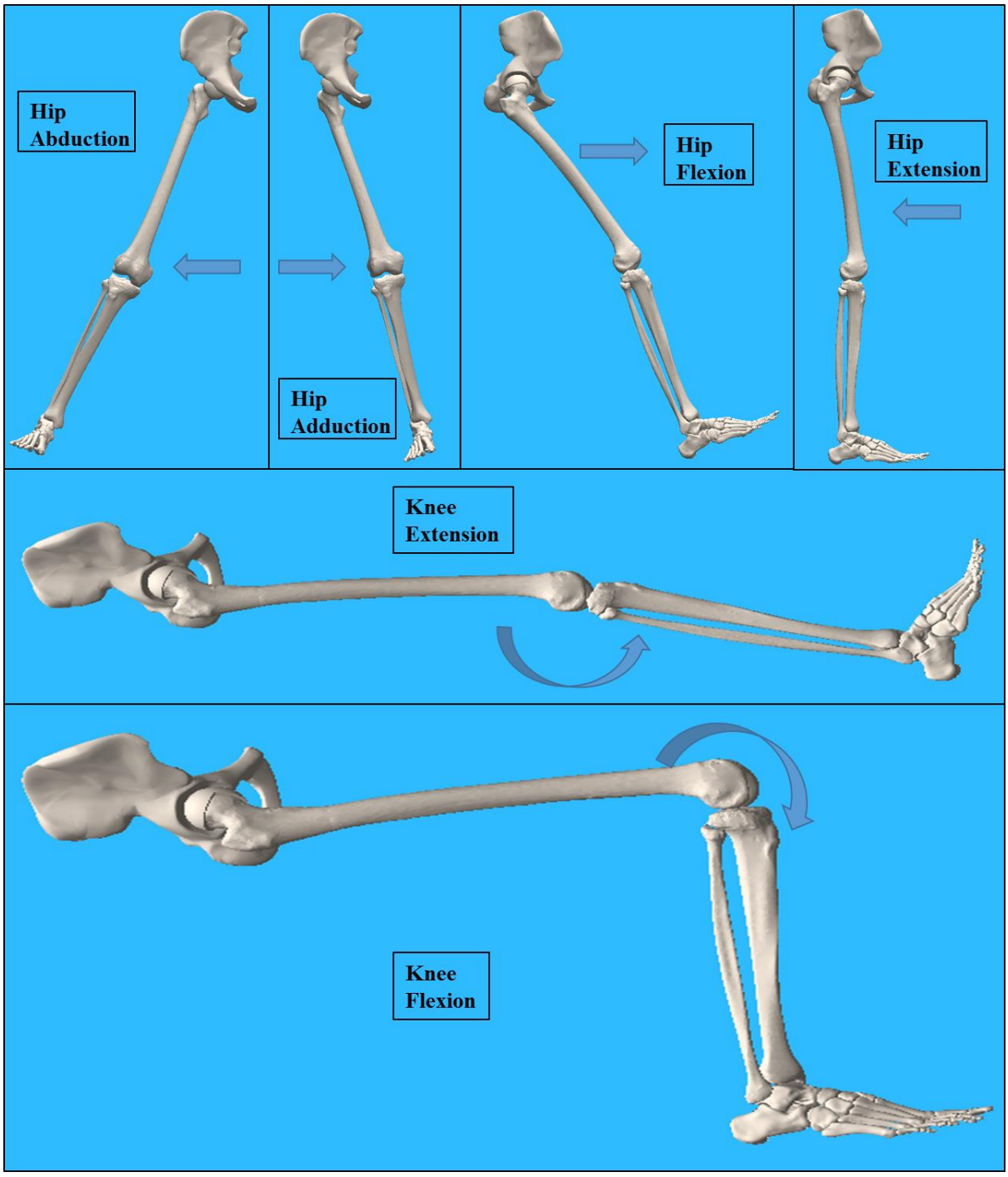

Figure 1-2: Anatomical Hip and Knee Joint Motions

1.3 Statement of Purpose

The principal goal of this dissertation is to understand the connection between reductions of subtle and severe dislocations, passive muscle forces and moments generated while the Pavlik harness is used during treatment. By understanding the kinematics and dynamics of developmental dysplasia of the hip, the use of orthosis to treat this condition can potentially be optimized and improved. To this end, the concept of personalized pediatrics will be implemented to develop a physical model of the lower limb of a ten-week old female infant. Next, adductor muscles will be modeled in the lower limb as action/reaction forces exhibiting passive behavior. Finally, the kinematics and dynamics will be analyzed using the Rigid Body Dynamics Method. With the use of a patient-specific model, subtle and severe dislocations presented in infants can be successfully elucidated. The outcome of the current dissertation will quantify the biomechanics of developmental dysplasia of the hip in infants, and will also suggest means to optimize the use of the Pavlik harness. In addition, results of this study will provide guidance to develop innovative new medical devices to successfully treat developmental dysplasia of the hip in the future. Moreover, the methodology used on this dissertation can be effectively implemented in several conditions where fractures, dislocations, and separations in the skeleton may occur. Such methods provide the flexibility of dislocating the hip joint, which to our knowledge, has not be done yet to investigate and optimize orthopedic rehabilitation.

1.4 Thesis Overview

The work developed on this dissertation is captured and arranged in six chapters. Following the introductory chapter, Chapter 2 presents an overview of developmental dysplasia of the hip

and hip biomechanics. Chapter 3 will then complement the groundwork started in Chapter 2 by providing details of skeletal muscle mechanics and describes related work on this field. In addition, Chapter 2 and Chapter 3 outline some of the major assumptions of this dissertation. The information on these two chapters is also detailed enough aiming to develop an understanding on readers without previous knowledge and experience in the field of bone and muscle mechanics. Following this background information, the specific features and methodology used to develop the patient-specific model of the ten-week old female infant will be presented in Chapter 4. To explain the particulars of the physics-based anatomical model, Chapter 4 is divided into several subsections. These subsections include the following subjects: the anatomical reconstruction; the anatomical assembly; the utilization of a passive muscle model; the implementation of the Rigid Body Dynamics Method; the lubrication of the hip joint; the anatomical model calibration; and the different dislocations studied. Chapter 5 presents the forces and moments that were quantified by elucidating the effects of the Pavlik harness on subtle and severe dislocations. Finally, Chapter 6 discusses the findings of this dissertation and summarizes the contributions. Moreover, this final chapter will include final remarks on future research directions related to improve the usage of the Pavlik harness and other orthosis.

CHAPTER 2: BIOMECHANICS OF DEVELOPMENTAL DYSPLASIA OF THE HIP

In order to understand the biomechanics of developmental dysplasia of the hip, a reasonable understanding of the condition is needed. To this end, this chapter presents two sections: section 2.1 will review and present detailed information of the etiology, pathoanatomy, pathophysiology, diagnosis, classification, and treatment of developmental dysplasia of the hip. A proper background knowledge of this condition will help to provide correct assumptions to effectively tackle an anatomical model that exhibits the mechanics of developmental dysplasia of the hip. Finally section 2.2 will present the biomechanics of the lower limb which aims to explain the mechanical factors behind this common condition and to provide means of proper mechanical modeling of the bony structure.

2.1 Developmental Dysplasia of the Hip

In general developmental dysplasia of the hip is an abnormal condition where hip joint dislocation, misalignment, and instability are present in infants. It has been stated that "congenital dislocation of the hip represents one of the most important and challenging congenital abnormalities of the musculoskeletal system" [5] and "in its severest form, developmental dysplasia of the hip is one the most common congenital malformations" [6]. It has been reported that clinical hip instability in newborn infants ranges from 1.6 to 28.5 per 1,000 [6] and 6 out of every 1,000 will require treatment [7]. Studies had also shown that developmental dysplasia of the hip was responsible for 29% of primary hip replacements in people up to age 60 years [8]. Although the condition may present after birth, most cases originate during fetal development,

thus it is commonly referred to as Congenital Hip Dysplasia (CHD). CHD is typically discovered during physical examination at birth and some common signs of dislocations are: asymmetrical hip abduction or asymmetrical limb lengths, hip click sounds, limited range of motion, and pain. Therefore, it is crucial to diagnose hip dislocations timely postnatally, and expedite the onset of treatment. Successful hip reductions in all cases must be achieved during the first few months of life as the anatomy is still in its developmental phase. In all cases, the success of the treatment is inversely related to the age at which treatment is begun, with success rates remaining the highest when the treatment is begun immediately after birth or within the first month, and declining after 9 months of age [9].

2.1.1 Terminology, Etiology, Pathoanatomy, and Pathophysiology

Formerly known as congenital hip dislocation (CDH) [10] or hip dysplasia, the terminology used to describe hip displacements or dislocations is controversial. The term "congenital' was previously used to describe dislocations or displacements due to genetics or mechanical factors affecting the fetus in utero and the term "dysplasia" was used to refer to irregular development of the femoral head, acetabulum, or both after the neonatal period [11]. Additionally, physicians in the past have favored the used of the term "congenital dysplasia' instead of the term "congenital dislocation" [12]. This preference in terminology was based on the fact that dysplasia better describes the morphological alteration of the hip. In addition, "dysplasia" refers to cases where there is partial contact between the acetabulum and the femoral head (subluxation) and cases where there is no contact between the acetabulum and the femoral head (dislocation). The latest term, developmental dysplasia of the hip was adopted to define

displacements or dislocations regardless of nature or time when the abnormal condition first appeared. Developing an understanding of the etiology, pathoanatomy, and pathophysiology of developmental dysplasia of the hip is relevant to the study of this dissertation. Thus, this section will present some of the factors that have been suggested to be main contributors of hip displacements or dislocations before, during, and after the neonatal period.

Early experiments have shown that it is possible to dislocate the hip in an embryo for the first time at 11 weeks old [13]. It has been suggested that there are critical periods during which the hip of a fetus is at risk of dislocation: the 12^{th} week, the 18^{th} week, and the final 4 weeks of gestation [14]. Additionally, packaging abnormalities at earlier stages of pregnancy may limit movement in the utero leading to dislocations. Experimental results have also suggested that breech presentation [5, 15], female sex [16-18], oligohydramnios [19, 20] , and primiparity [21] are major risk factors. Furthermore, the risk is believed to increase when a breech-presenting child is delivered vaginally rather than by caesarean section [3, 22]. Dislocation vulnerability before birth is known to be caused mainly by the acetabular-capacity and depth relative to the femoral head. Experimental studies have suggested that the acetabulum becomes shallow as birth approaches [23]. This depth difference between a normal hip and a shallow hip affects the articular range of hip motion as seen in Figure 2-1.

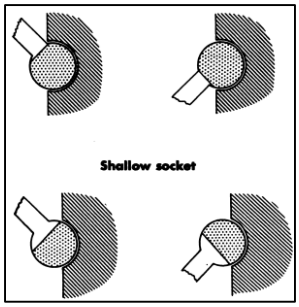

Figure 2-1: Representation of a Normal Socket (Top) and Shallow Socket (Bottom) [23]

Additionally, experimental results have indicated that the coverage provided by the acetabulum to the femoral head decreases drastically before birth as seen in Figure 2-2. This finding in particular provides a possible explanation for dislocations or displacements in the infantile hip caused by the reduced contact between the femoral head and the acetabulum before and during the neonatal period. This type of dislocation is known to be the most severe form of developmental dysplasia of the hip since it will cause abnormal development of the lower limb.

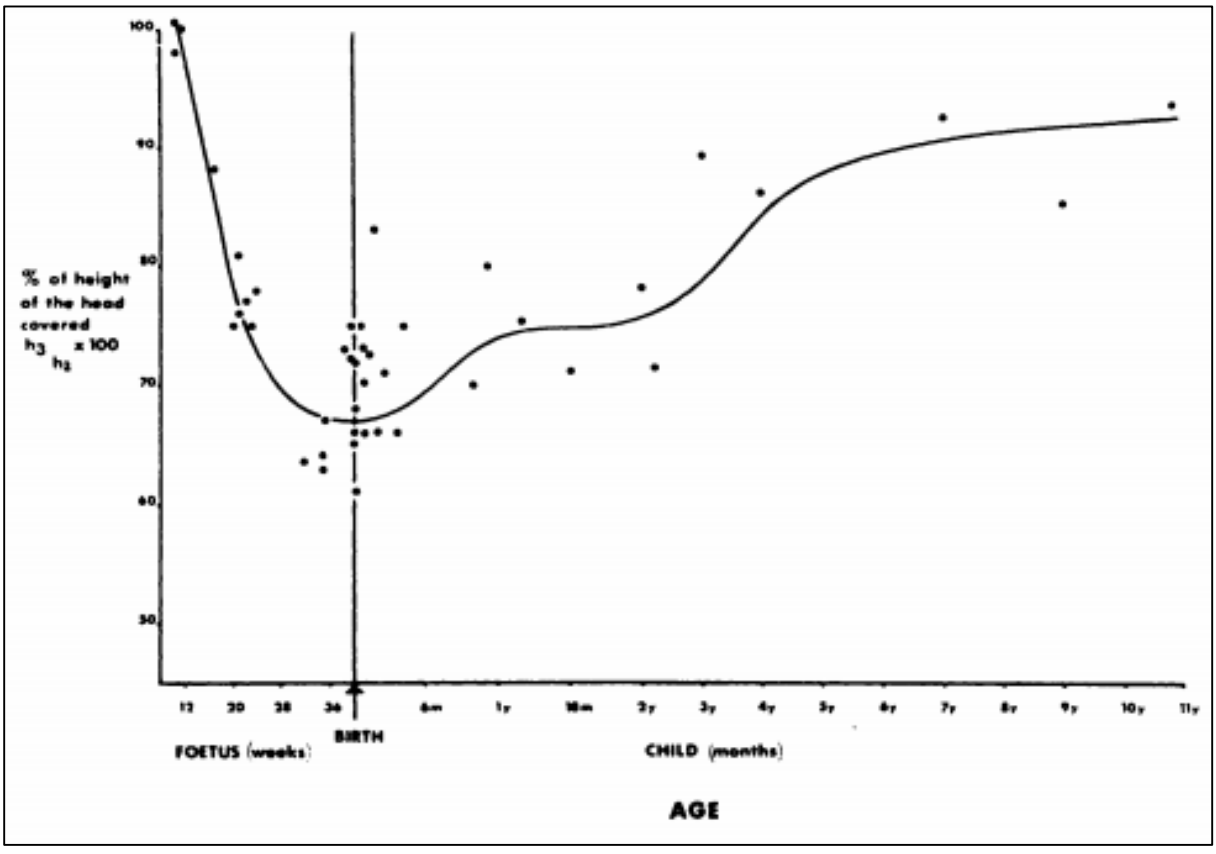

Figure 2-2: Proportional Changes of the Femoral Head Covered by the Acetabulum [23]

Contrastingly, anatomic experiments in Africans have shown that the acetabulum remains deeper before birth providing more coverage to the femoral head. Thus, confirming the demographics of developmental dysplasia of the hip where incidence is almost nonexistent in

African neonates [24]. This particular study has lead clinicians to perform anatomical experiments to understand how geographic and ethnic factors influence developmental dysplasia of the hip in infants. It has been suggested that racial and geographical incidence is mainly caused by positioning of the neonate. Particularly, studies had being focused on various swaddling methods around the world. Reports have indicated that swaddling during the first months of life may increase dislocation risk based on usage configuration. For instance, it is known that Africans, Chinese, and Eskimos groups swaddle newborn infants to maintain hips in abduction and flexion as seen in Figure 2-3. Such configuration mimics the ones found in typical non-surgical harness/braces used to treat developmental dysplasia of the hip. Moreover, incidences recorded on these groups have been reported to be remarkably low.

Figure 2-3: Swaddling in African (Left), Chinese (Center), and Eskimo (Right) Groups [5]

Conversely; for Italian and Native Indian groups, who swaddle newborn infants maintaining the hip in extension and adduction as seen in Figure 2-4, incidences are remarkably

high. Furthermore, swaddling is controversial since its use has been linked not only to developmental dysplasia of the hip but also to sudden infant death syndrome (SIDS) [25].

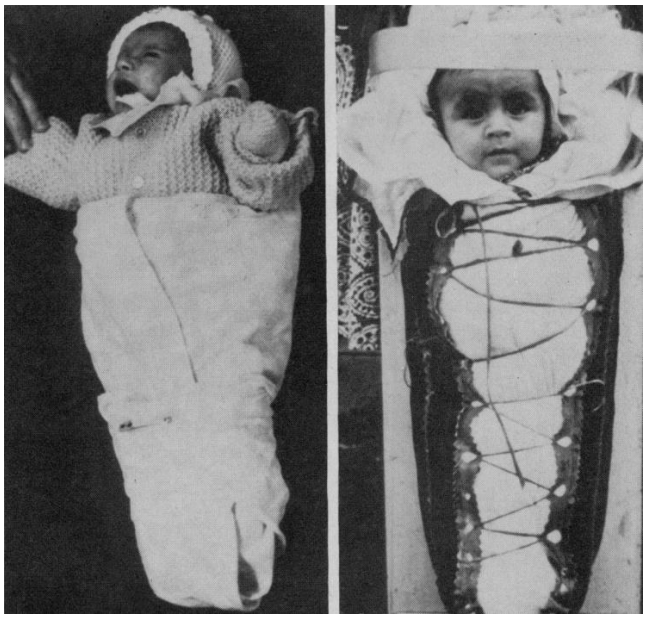

Figure 2-4: Swaddling in Italian (Left) and Native Indian (Right) Groups [5]

Furthermore, fully dislocated hips may present well developed false acetabulum and bilaterality [26]. A severed dislocated hip with a well develop acetabulum will have a great impact in adult life by increasing the risk to develop degenerative joint diseases.

For cases presented at birth, Barlow reported that one in sixty infants will show sign of instability and 12% will require treatment [27]. Several cases have been reported where hip appeared to be normal at birth but dislocated during the postnatal period [28, 29]. Incidences after birth are believed to be caused mainly by postnatal positioning. Within the newborn population affected with any type of instability, some may be reduced without treatment, some develop may develop subluxation and some may progress to a dislocation.

2.1.2 Diagnosis, Classification, and Treatment

Physicians in the past believed that an examination of a newborn will successfully provide a diagnoses for a dislocated hip. However recent studies have determined some types of dislocations go by undetected at birth and some may occur in the neonatal period or later. The U.S. Preventive Services Task Force has also stated that: "evidence is insufficient to recommend routine screening for developmental dysplasia of the hip in infants as a means to prevent adverse outcomes" [30]. Nonetheless, physical examination is recommended during regular infants check-ups. As presented in the last section developmental dysplasia of the hip could appear at any point after birth and is of paramount importance to keep track of hip joint development. A simple visual way to detect dislocations in newborns is by looking for asymmetry patterns in the lower limb of a neonate. Physical examination is always performed in the neonatal period and two of the most common clinical test are the Ortolani [31] and Barlow [27] maneuvers. The Ortolani and Barlow maneuvers, have become the "gold standard" techniques to asses hip stability on 3 months old infants or younger. The Ortolani procedure is performed by gently abducting the leg with the hips flexed at 90° and applying an upward force through the greater trochanter as seen in Figure 2-5. An Ortolani positive test will feature a palpable "clunk" sensation representing the reduction of the dislocated hip. In general, a positive Ortolani test indicates a reducible dislocation while a negative Ortolani test indicates an irreducible dislocation. On the other hand, the Barlow procedure is performed by adducting the leg with the hips flexed at 90° and gently pushing the knee as seen in Figure 2-5. A Barlow positive test will feature a palpable "clunk" sensation and will force the femoral head out of the acetabulum confirming hip dislocation.

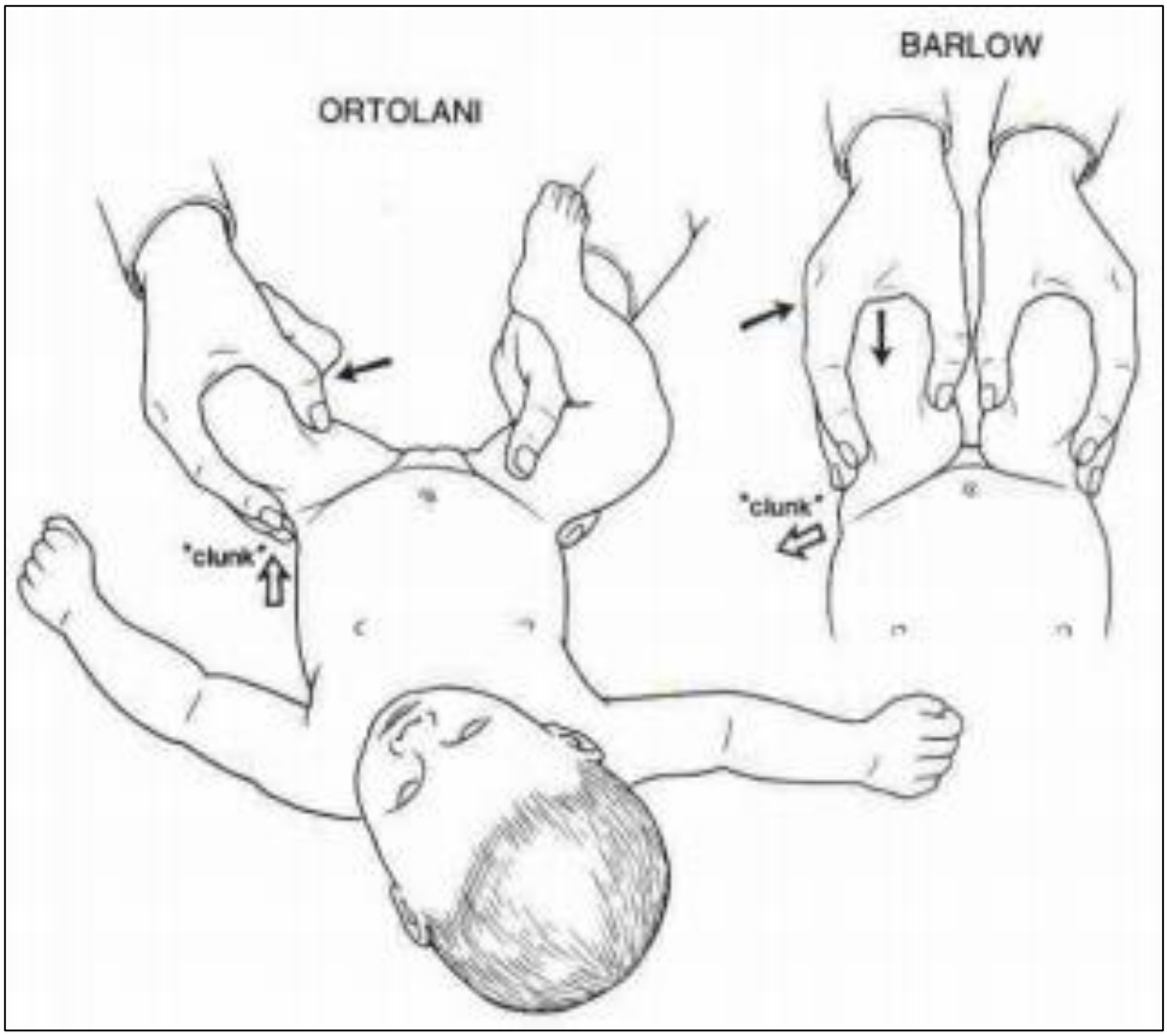

Figure 2-5: Ortolani and Barlow Maneuvers [32]

From 3 to 12 months the use of both maneuvers is not recommended due to lack ligaments and capsular laxity. For these older infants, a visual check is performed by the pediatric physician by placing the infant supine on a firm table and then abducting both hips at the same time to check for any asymmetries as shown in Figure 2-6.

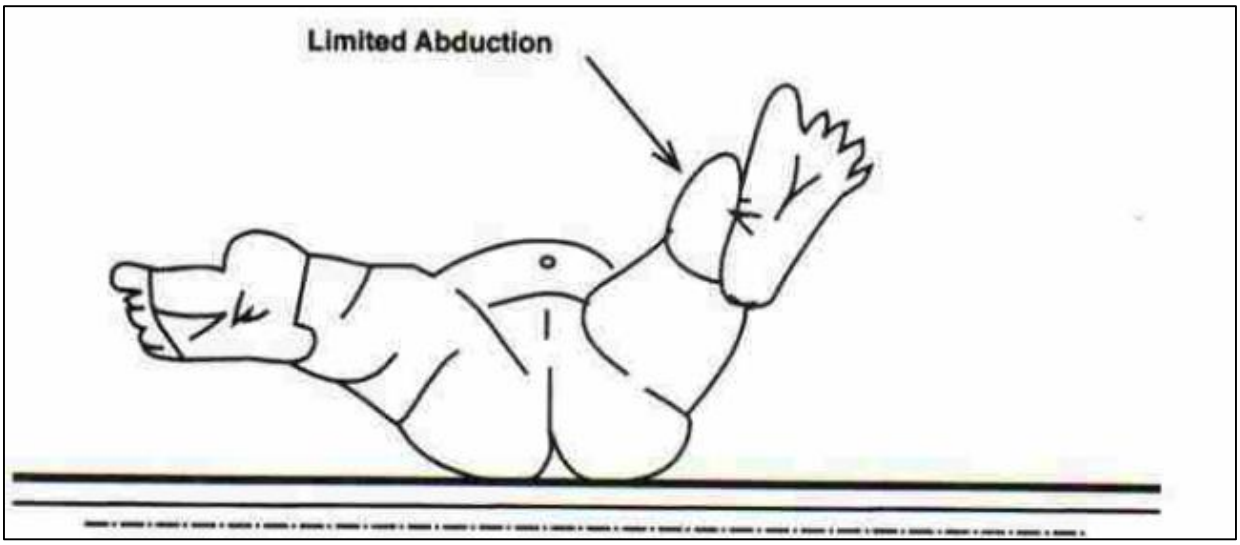

Figure 2-6: Limited Abduction Left Infant Hip [32]

Radiographic evaluation is the standard whenever it comes to diagnoses. However, it is known that during the neonatal period is difficult to interpret radiographs due to cartilaginous regions where the femoral head-acetabulum correlation cannot be determined. Graf proposed the use of ultrasound [33] to diagnose developmental dysplasia of the hip and suggested the use of four sub-types of displacements or dislocations. However, it has been reported clinical ultrasound usage may provide false-positive results [34]. Tönnis presented a method to classify developmental dysplasia of the hip severity by assessing the location of the ossific nucleus using radiographs [35]. Additionally, the International Hip Dysplasia Institute has developed a new radiographic classification using the Hilgenreiner's line (H-line), Perkin's line (P-line), Diagonal line (D-line), and H-point as defined is Table 2-1 and shown in Figure 2-7.

Table 2-1: International Hip Dysplasia Institute (IHDI) Classification using Radiographic Measurements [36]

Radiographic Measurement	Description
Hilgenreiner's line (H-line)	The single line drawn through the top of the triradiate radiate cartilage bilaterally
Perkin's line (P-line)	Perpendicular line from the superolateral margin of the acetabulum
Diagonal's line (D-line)	45 degree line from the junction of H-line and P-line
H-Point	Midpoint of the superior margin of the ossified metaphysis

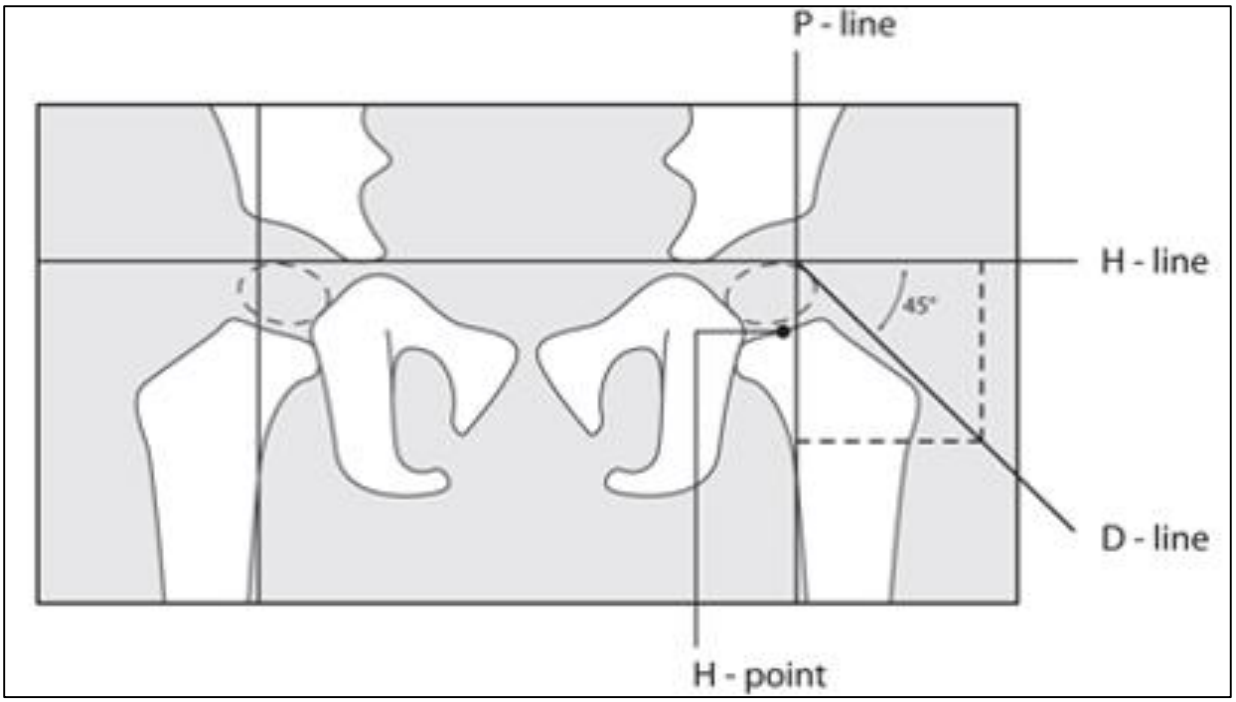

Figure 2-7: Radiographic Measuring Parameters for Severity Classification [36]

The International Hip Dysplasia classification uses the position of the proximal femoral metaphysis to define the severities as follows: Grade 1, the ossification center of the capital

epiphysis is medial to the Perkin line; Grade 2, the ossification center of the capital epiphysis is lateral to the Perkin line; Grade 3, the ossification center of the capital epiphysis is at the level of the supero-lateral margin of the acetabulum; and Grade 4, the ossification center of the capital epiphysis is above the level of the supero-lateral margin of the acetabulum as seen in Figure 2-8.

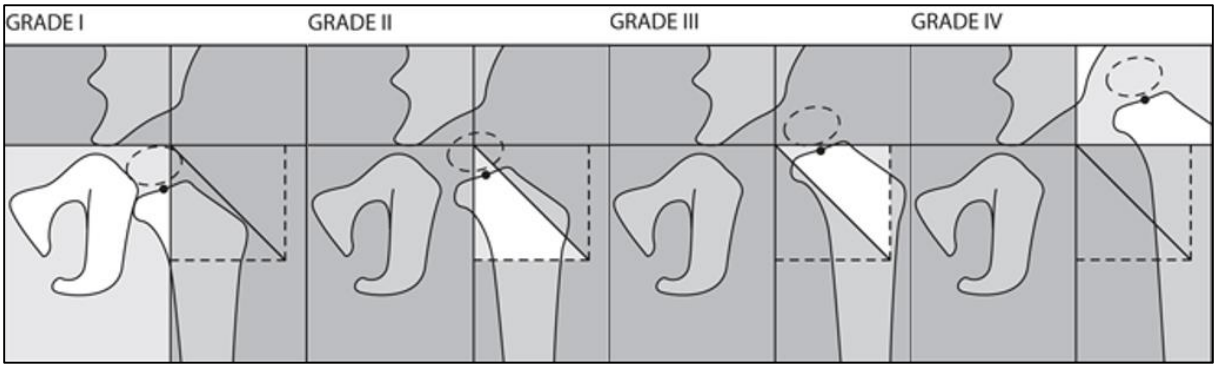

Figure 2-8: International Hip Dysplasia Dislocation Grades [36]

This particular classification has shown to be more reliable than the commonly used Tönnis classification [36]. Both classifications identify severity of dislocation as Grades 1 through 4 with Grade 4 being the most severe dislocation. However, the Tönnis classification can only be applied after ossification of the femoral head at approximately the age of six to twelve months. The International Hip Dysplasia Institute method to classify dislocation severity may be more useful since it can be applied at any age. In both classifications the Grade 4 dislocations are characterized by the center of the femoral head being displaced above the level of the supero-lateral margin of the acetabulum.

After proper assessment of developmental dysplasia of the hip, the next step is to treat the disorder. The main outcome expected after treatment is to achieve reduction of the hip assuring proper lower-limb development. Standard protocols have been established to treat infants depending on instability, dislocation severity, and age. In general, developmental dysplasia of the

hip could be treated using non-surgical and surgical treatment methods. A non-surgical treatment method is recommended for infants less than 6 months of age when it is known infant ligaments are lax, and the acetabular labra comprise malleable and elastic cartilage. Such methods aim to accomplish reduction by maintaining the hips in flexion and abduction as seen in Figure 2-9. By analyzing muscle forces exerted in flexion and abduction, this particular positioning may explain mechanical reduction of the hip. The line of action generated by this posture may have a favorable effect towards reduction in subtle dislocations when the femoral head lies near the acetabulum rim. Contrastingly, if the femoral head lies posterior to the acetabulum, the line of action may contribute to entrapment of the femoral head aggravating the already dislocated hip. These techniques involve the use of harness or braces such as the Pavlik harness [37], the Hoffman-Daimler brace [38], the Von Rosen splint [39], the Frejka pillow, Spica cast, semirigid hip orthosis [40] and traction methods, to name a few.

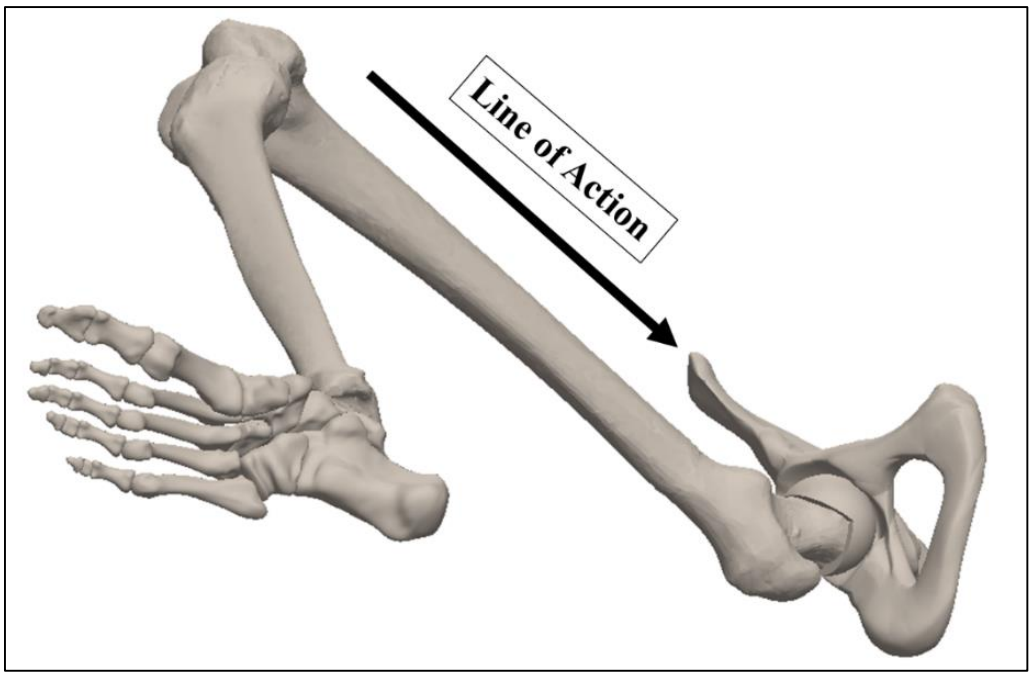

Figure 2-9: Hips Placed in Flexion and Abduction

Surgical treatment methods include the use of closed reduction, open reduction, pelvic osteotomy, and femoral osteotomy procedures. Osteotomy procedures are performed in children older than 2 years old and involve the reshaping of either the pelvis or the femur to accomplish reduction. Closed reduction is a minimally invasive procedure, commonly used between the ages of 3 and 24 month, where the hip is physically manipulated to enable reduction using real-time x-ray viewing. When unsuccessful, a closed reduction is usually followed by an open reduction procedure where surgery is performed in the infant. The surgery is commonly performed in infants at 6 months of age and older and the main purpose is to remove obstructing tissue that may prevent reduction of the hip. A cast is often needed by the open reduced hip to guarantee hip alignment and development. Avascular necrosis, which affects blood supply to the bones, has been reported to frequently appear after open reduction procedures in about 60% of surgical reduced hips [41]. Thus, non-surgically methods are preferred instead of open surgery reductions that may lead to complications such as femoral osteonecrosis and redislocation. Figure 2-10 presents a typical mapping for treatment of an infant before 6 months of age showing possible procedures as a function of age and dislocation severity. Some features reported due to dislocations in children after birth are: evident asymmetry of thigh creases, difficulty in crawling, limping, walking on tiptoe, and dragging one leg [6]. In adolescence, patients with developmental dysplasia of the hip may experiment discomfort or pain when walking. If left untreated, this condition could progress into diseases such as osteoarthritis, osteonecrosis, ochronosis, and hemochromatosis, to name a few.

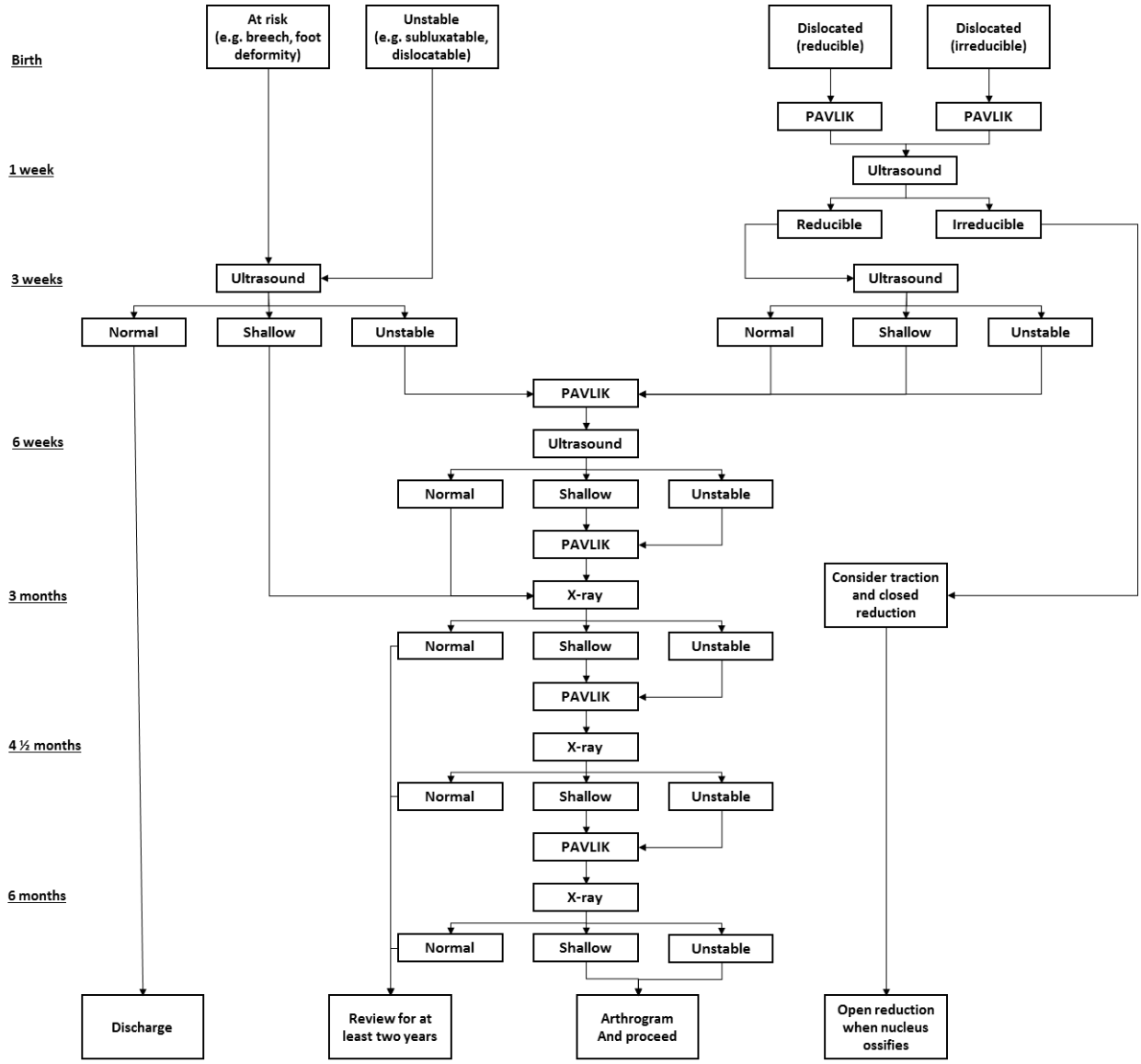

Figure 2-10: Developmental Dysplasia of the Hip Treatment Mapping in the First 6 Months of Life [4].

2.1.3 Treatment with the Pavlik Harness

Based on dislocation severity, the Pavlik harness, which is a standard non-surgical treatment method designed to maintain the hips in abduction and flexion simultaneously [9, 42] as seen in Figure 2-11, might be used to avoid surgery and bring the femoral head back to the acetabulum (reduction). The Pavlik harness has become the standard to treat developmental dysplasia of the hip during the first six months since it enables spontaneous mechanical reduction without rigid fixation and it also is a cheaper alternative compared to other harnesses or braces.

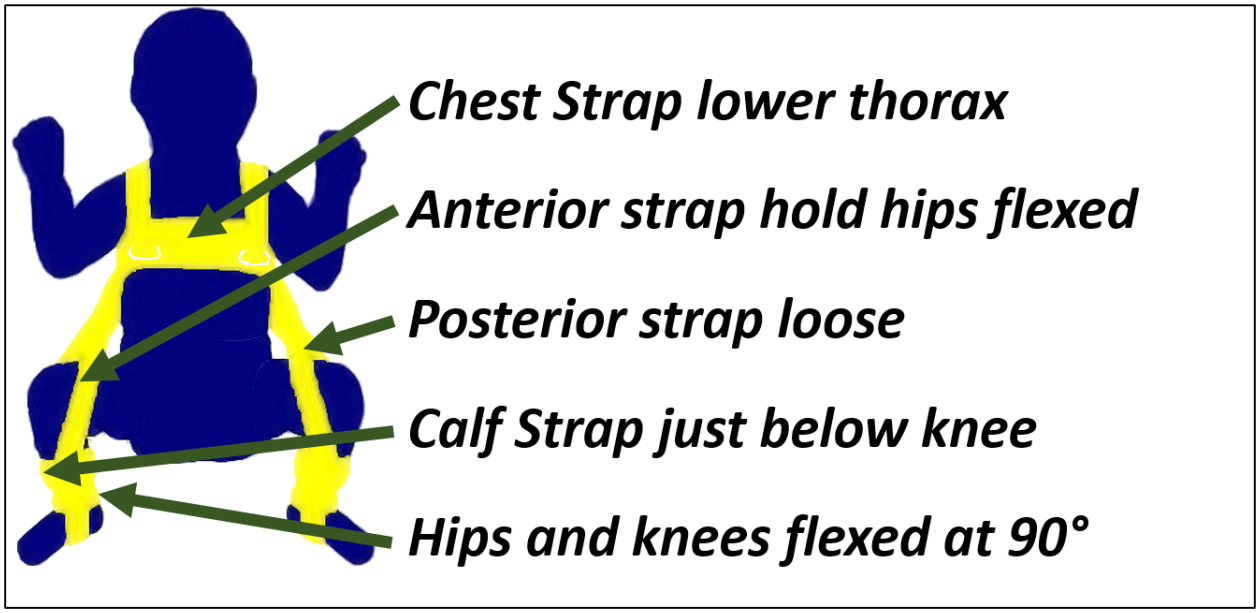

Figure 2-11: Typical Pavlik Harness Configuration

To improve the use of the Pavlik harness, Ramsey [42] proposed a safety zone, avoiding adduction less than 35°, which will further severe dislocation, or abductions bigger than 75°, which may increase the risk of avascular necrosis. Regardless of using this type of protocol; the harness is not always effective, and its effectiveness often depends on physician expertise, or trial-error procedures. Treatment success with the harness is inversely related to initial dislocation severity,

and age onset of treatment [43]. It has been found that harness treatment fails in approximately 15% of cases following birth [44-47], and incidence of failure doubles when treatment begins after three weeks of age [48]. Figure 2-12 shows experimental results where it was shown that treatment on infants aged seven weeks and under had a higher rate of success than those aged eight weeks and over [49].

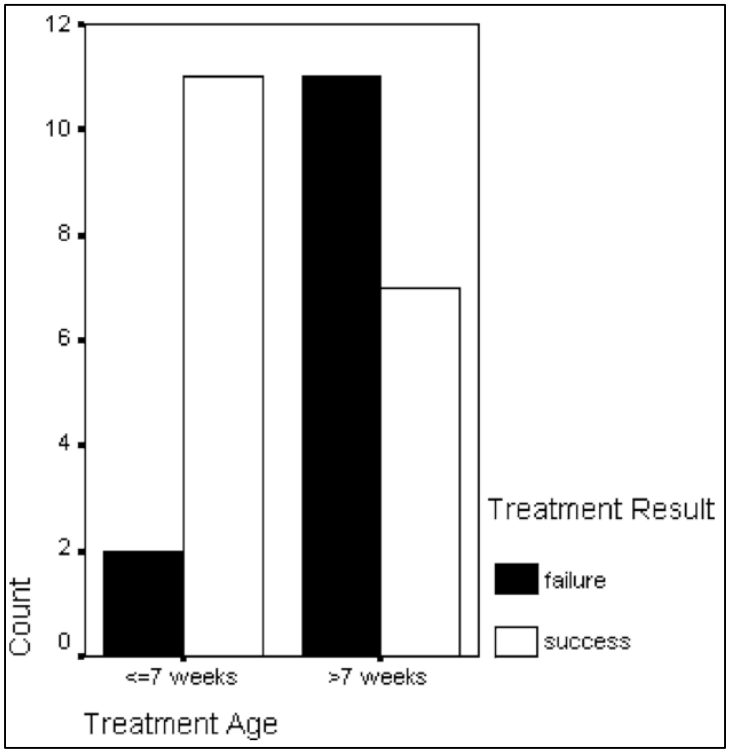

Figure 2-12: Relationship Between Age and Treatment Success [49].

Statistically, it has been shown that for IHDI Grades 1-3, reduction rate is 92% while for Grade 4 reduction rate is approximately 2% [50]. Clinical reports and previous research has indicated very low success of the harness for more severe grades of hip dislocation [40, 49, 51]. Experimental studies using the Graf classification had shown that infants with type IIC, IID, or III, hips had a higher rate of treatment success than infants with type IV hips [49] as seen in Figure 2-13.

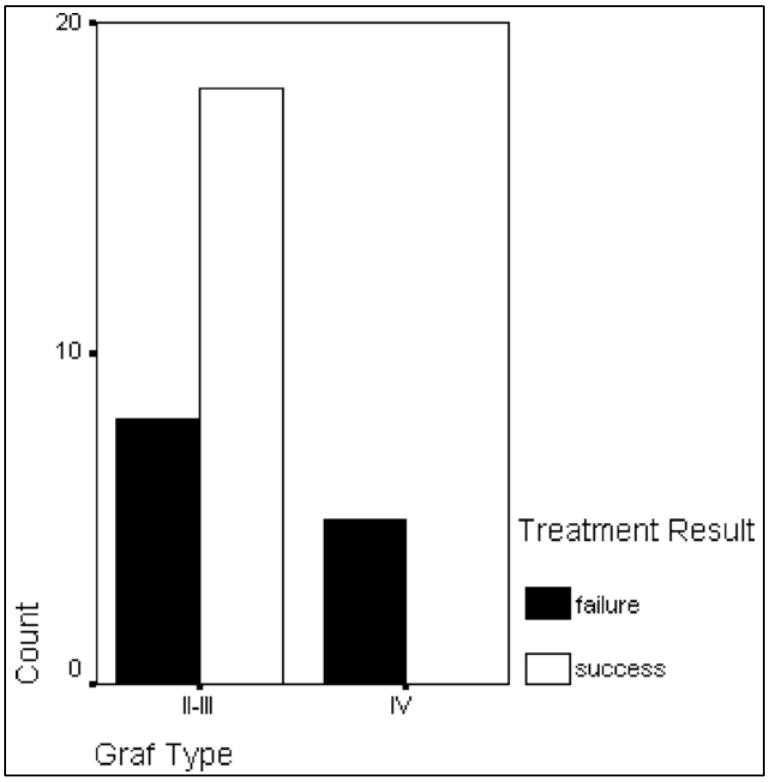

Figure 2-13: Effect of Graf Type on Treatment Results [49].

Additionally, prolonged treatment of inadequately reduced hips carries deleterious consequences [45, 52], hence accurate and timely reduction is needed. Moreover, excessive abduction could provoke avascular necrosis of the femoral head. The incidence of failure is the essence and the motivation of this dissertation. Studies have reported failures but there is no work, that I am aware of, that has quantified the mechanics of reduction of the harness. Thus, the key to a successful treatment is to quantify force and moment muscle contribution on dislocated hips to be able to enhance and optimize the use of these methods and devices.

2.2 Lower-Limb Bone Biomechanics

Mechanically, the hip joint represents a ball and socket joint where the connection between the femoral head and the acetabulum in the pelvis provides stability in the human body. Acting in concert with their corresponding skeletal muscles, the hip joint enables locomotion providing a wide range of motion. Extensive work has been done to quantify forces and moments during routinely physical activities. Specifically, we are interested in covering the hip joint physiology and pathology factors that will affect the biomechanics of the lower limb when developmental hip dysplasia is present.

The biomechanics of the lower limb has been studied in the past to understand abnormalities such as osteoarthritis and to plan orthopaedic procedures using analytical and imaging techniques [53-56]. Maquet, based on Pauwels' theories [56], studied hip dysplasia mechanics on adults and children while walking [53]. He used the center of gravity of the mass of the body supported by the hip (S_s), the force exerted by the mass of the body supported by the joint (K), the lever arm of K (h'), the force exerted by the abductor muscles (M), and the lever arm of M (h) to find the force transmitted across the joint (R) as seen in Figure 2-14. Additionally, he looked at different cases of dislocation and observed that besides the muscular imbalance caused by dislocations, the articular pressure in the hip increases and could potentially increase the risk to develop osteoarthritis. Bombelli followed a similar approach using a radiographic analysis [55]. He suggested that mechanical forces exerted in the hip joint can be estimated using radiographs and comparing deviation of force magnitudes and directions from healthy hips to assess different types of osteoarthritis. Altogether, these studies indicate that hip mechanics are governed by the anatomical architecture of the hip joint bones and the response of the skeletal muscles.

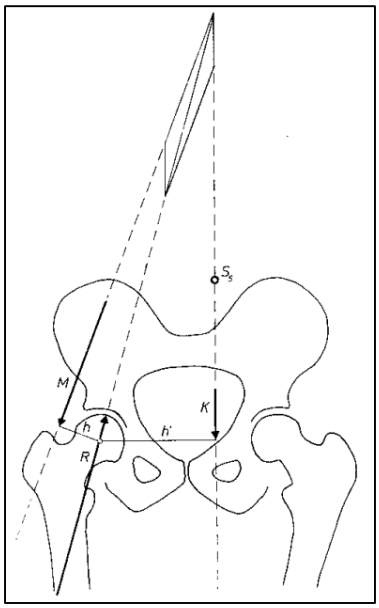

Figure 2-14: Forces Exerted on a Loaded Hip while Walking [53, 56]

The femoral head shape has been identified as one of the contributors that could potentially affect the biomechanics of the hip joint. However, anatomic studies have shown that the shape of the femoral head is nearly hemispherical around the time of birth as seen in Figure 2-15. These results will allow us later on to use the assumption that for neonates less than twelve week old the femoral head remains spherical during hip joint locomotion.

Figure 2-15: Changes in the Shape of the Femoral Head in Relation to Age. From Left to Right: 21-week fetus, 30-week fetus, Premature Newborn, 2 Years, 4 Years [23].

In addition to femoral head sphericity, physicians have investigated femoral head anteversion in infants with developmental dysplasia of the hip. Femoral head anteversion is denoted by the torsion or twist of the femoral head. To define femoral anteversion angle, Murphy's sound method [57], which has been set as the standard measuring technique, has been adopted for the work developed on this dissertation. He defined the long femoral (FA) axis using the center of the knee (K) and the base of the femoral neck (O); and the femoral neck (FNA) axis using the center of the femoral head (H) and the center of the base of the femoral neck (O). For this method the condylar axis (CA) is defined as an axis that is intersected by the center of the knee (K) and is parallel to the axis formed by the posterior aspect of the medial condyle (M) and the posterior aspect of the lateral condyle (L). Subsequently, the condylar plane (CP) is defined by the intersection of the condylar axis (CA) and the femoral axis (FA). He then defined the plane of anteversion (AP) as the plane containing both the long femoral axis (FA) and the femoral neck axis (FNA). Finally, the angle of anteversion (θ) is the angle defined between the condylar plane (CP) and the plane of anteversion (AP) as seen in Figure 2-16.

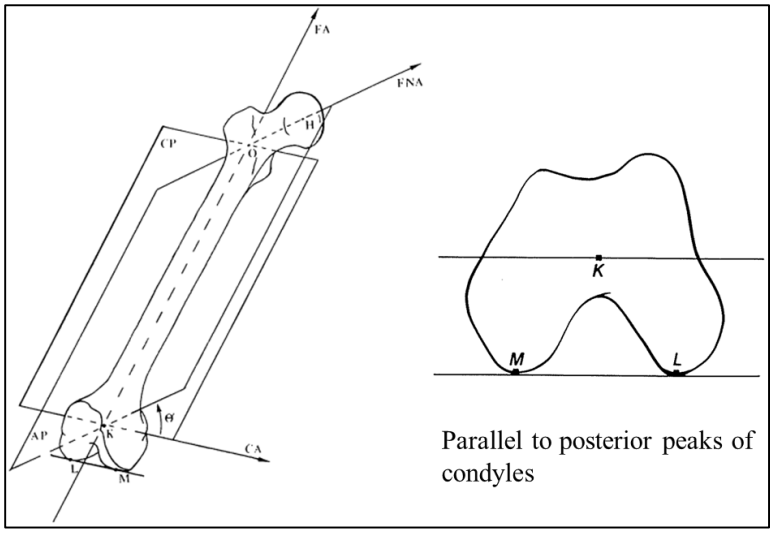

Figure 2-16: Murphy's Method for Measuring Femoral Anteversion Angle [57]

Once properly defined, the femoral anteversion angle is measured clockwise. A counterclockwise angle will yield to femoral neck retroversion as seen in Figure 2-17.

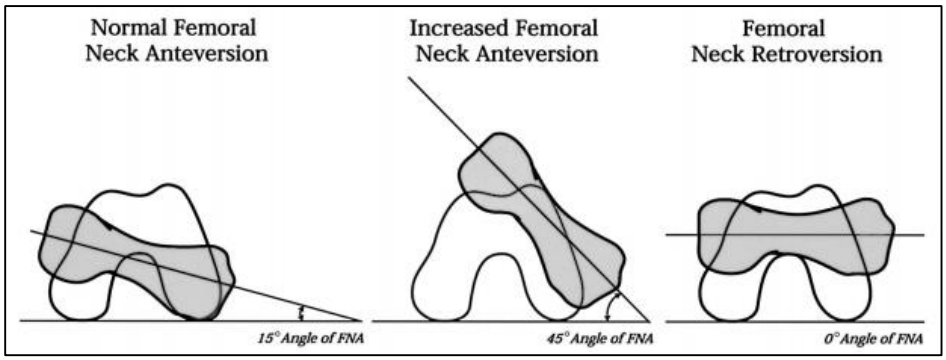

Figure 2-17: Femoral Anteversion Classification: Normal (Left), Increased Angle (Center), Retroversion (Right) [58].

Anatomical studies have shown that for newborns the femoral anteversion angle average falls around 31° [59] and it has been suggested that angle values that fall outside the average may contribute to different orthopedic problems [58]. In addition, these studies have shown that anteversion angle is greater for dislocated hips than for healthy hips. Furthermore, it is known that this angle is reduced with age but remains high for dislocated hips as seen in Figure 2-18.

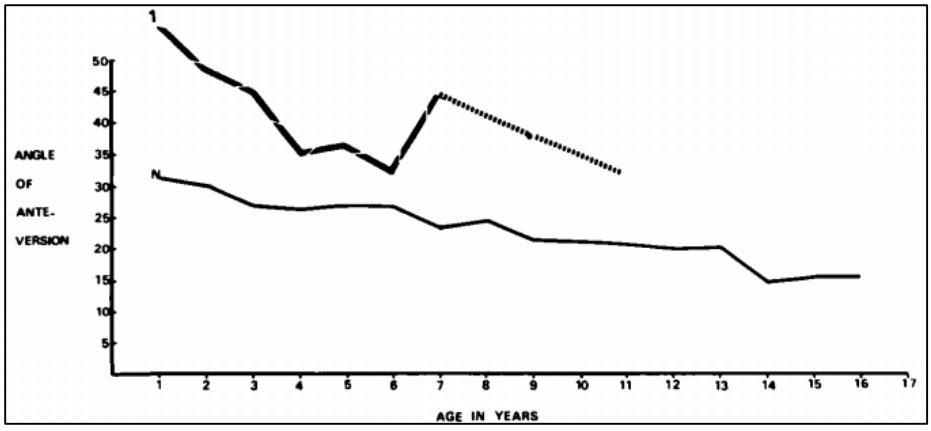

Figure 2-18: Femoral Anteversion in Relation to Age: (1) Hip with Developmental Dysplasia of the Hip and (N) Healthy Hips [59].

Overall, research related to the femoral anteversion angle have suggested that forces and moments developed during hip motion may be affected by the changes of this angle, but these effects have not been quantified. Therefore, it is relevant for the work developed on this dissertation to investigate how femoral anteversion angle may affect hip reduction success rate.

Bones are composed of cortical bone, trabecular bone, and cancellous bones. All these regions within the bone are critical for accurate modeling of hip mechanics. However, for the work developed in this dissertation, mechanical properties of the different regions of the bone are not accounted for and therefore not discussed further. Although relevant for biomechanics study, it is assumed that deformations in infant bones are very small compared to the deformations of skeletal muscles. Thus, bones are modeled as rigid bodies. In continuum mechanics, physical bodies are classified as either rigid or deformable. A deformable body will present elastic behavior and a rigid body, which is a mathematical and physical idealization, will not deform and will maintain a constant distant between any two points within the body. This idealization will hold its validity for very small deformations relative to the object size.

Having described hip biomechanics and developmental dysplasia of the hip, the next chapter will introduce the mechanics of skeletal muscles. In conjunction, Chapter 2 and 3 should provide sufficient information to successfully construct a neonate model to elucidate the biomechanics of developmental dysplasia of the hip.

CHAPTER 3: MECHANICAL BEHAVIOR AND MODELING OF SKELETAL MUSCLES

The previous chapter provided essential details of lower limb bone biomechanics, but in order to properly elucidate the biomechanics of developmental hip dysplasia, a modest understanding of muscle mechanics is needed. After all, within the human body, the kinematics and dynamics of locomotion are governed by muscle responses. In the human body, muscle tissues are categorized in three types: skeletal, cardiac, and smooth. Skeletal muscles or "voluntary muscles", which provide global mobility by acting in concert, are bundles of muscle tissue controlled by the neuro-central system and are attached to the bony skeleton. Cardiac muscle, often referred as "involuntary muscle", is only found in the heart and it is fascinating in nature since it is the only tissue that can contract without stimulation of the neuro-central system. Smooth muscle, also referred as "involuntary muscle", is found in the walls of certain organs and their function is to force continua through biological channels. The work developed on this dissertation to model the biomechanics of developmental dysplasia of the hip mainly deals with the forces and moments developed by muscles in the lower limb. Thus, this chapter will be focused on the analysis and study of skeletal muscles in the lower limb of the human body.

The biomechanics of the skeletal muscles has been studied and explored by several authors using novel approaches. Muscle biomechanics has been explored since the Renaissance when Giovanni Borelli [60] started investigating animal movement using machine analogies and mathematics as seen in Figure 3-1. For instance, Borelli linked heart behavior to the one observed in a piston allowing him to derive the elastic behavior in arteries. It is important to acknowledge that studying muscle mechanics has various limitations mainly due to the complexity of the

muscle-tendon unit. There are a lot of variables and limitations, which has made researches take particular approaches when it comes to the understanding of muscle mechanics. Vast research has been done in the area of muscle mechanics, but these studies are scattered and most of it has not been fully organized yet.

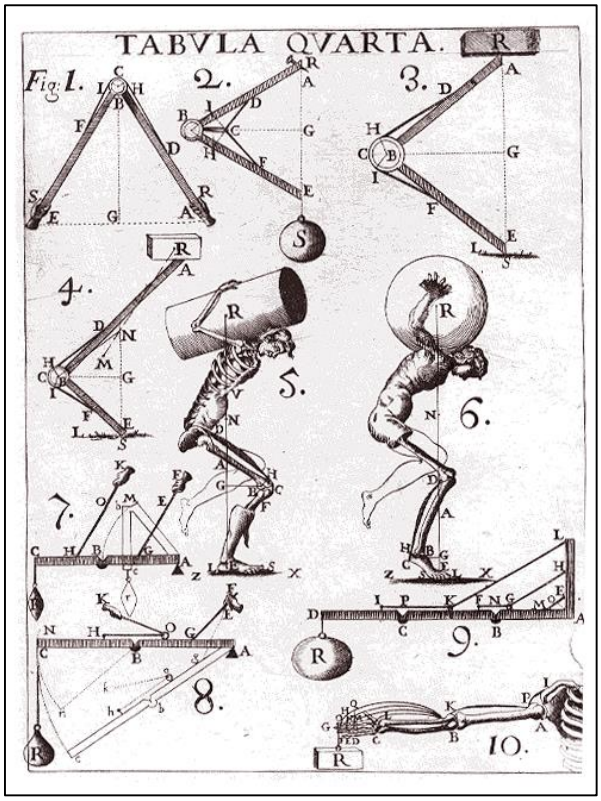

Figure 3-1: Borelli's Classic Work on Muscle Mechanical Behavior [60].

The purpose of this section is to provide a comprehensive analysis of muscle functionality and its structure based on previous research. Section 3.1 addresses muscle anatomy and the significance of mechanical features within skeletal muscles and also emphasizes skeletal muscle functionality. Section 3.2 will present various methods that have been used to realistically capture the mapping of a muscle path. Finally; section 3.3 will present the mechanical modeling of muscles and specifically it will introduce the use of Hill's muscle model, which has become the standard

for studies of muscle biomechanics. In addition, the last section of this chapter will also establish the basis to accurately reproduce skeletal muscle behavior action under passive tension. Muscle passive behavior, commonly known as relaxation, has been treated using distinct constitutive models developed which will be emphasized in the last section of this chapter. By understanding the behavior of relaxed muscles, scientists have been able to successfully simulate complex muscle systems and study muscle processes associated to muscle damage and/or fatigue, as well as muscle pathologies. Skeletal passive muscle response is of paramount importance on this dissertation, as it will be explained later on this chapter, and precise force and moment quantification is needed to elucidate the biomechanics of developmental dysplasia of the hip.

3.1 Skeletal Muscle Anatomical Structure and Physiology

This section will present biomechanically relevant anatomical features of skeletal muscles, which are necessary to understand force generation and movement in the human body. Mechanically, muscles can be considered biological motors which exert force and produce mechanical work, where the coupling of muscles and tendons is modeled as force transmitters and shock absorbers. The architecture of skeletal muscle exhibits important characteristics at multiple scales and can be studied at the microscopic and macroscopic level. In general muscles are made up of fiber bundles, called fascicles, and muscle fibers are muscle cells made up of small myofibrils which contain filaments.

At the microscopic level muscle fibrils or myofibrils, which are composed of serially connected elements called sarcomeres, represent the main mechanism of total muscle contraction. A sarcomere is the smallest contractile unit and is composed of a thin and a thick filament as shown

in Figure 3-2. Muscle contraction is then caused trough a chemical reaction produced by stimulation of the neuro-central system initializing the cross-bridge cycle, with the heads of the myosin (thick filament) connecting to the actin (thin filament). Later on this chapter, the mechanism of voluntary contraction will be explained to expose the concept of activation in skeletal muscles.

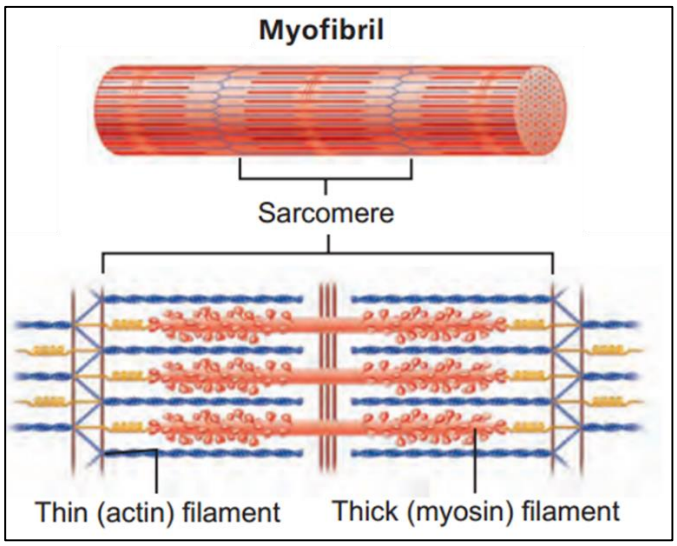

Figure 3-2. Myofibril and Sarcomere Architecture [61].

At the macroscopic level, the muscle fibers arrangement in skeletal muscles is responsible for loads that are mechanically transferred in the musculoskeletal system. In general this arrangement is composed of skeletal muscle tissue, nervous tissue, blood, and connective tissue. Particularly, connective tissue, which is made of collagen, adds the needed strength to keep muscles together. The network of connective tissue in the skeletal muscle is comprised of the epimysium, the perimysium and fascicle, the endomysium, and the fascia. Additionally, two other relevant connective tissues are the tendon, which is known to store potential energy and connects the skeletal muscle to the bone, and the aponeurosis, which connects external tendon to muscle

fiber and connective elements within the muscle fiber. A general representation of the muscle elements arrangement and its architecture is provided in Figure 3-3. Macroscopic modeling of skeletal muscle lays the foundation of the work developed on this dissertation as it can describe skeletal muscle response in a relaxed state.

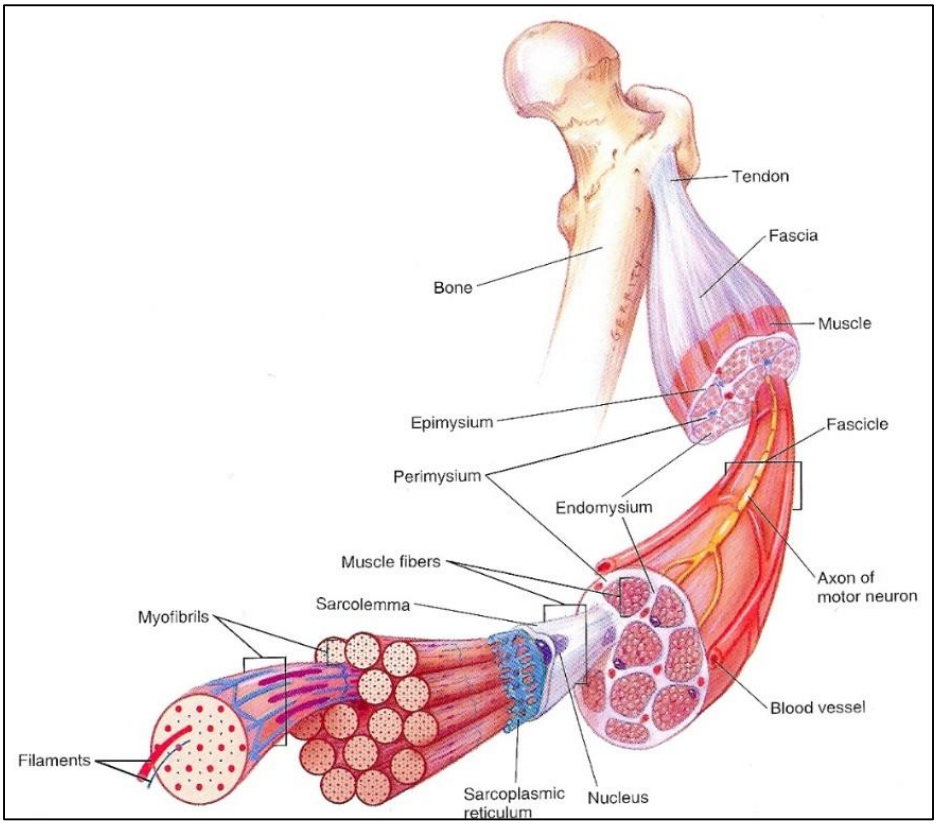

Figure 3-3: Muscle Structural Elements [62].

Defining muscle attachments also has mechanical relevance in force and moment generation. Muscle attachments can be defined either as origins or insertions and mechanically they can be model as points, lines, or surfaces. The immovable end of the muscle is designated as the origin and the movable end as the insertion. During skeletal muscle contraction, the insertion pulls towards the origin. For the lower limb, origins are located in the pelvis and insertion in the femur and tibia.

Another important muscle characteristic required for the studies on this dissertation is the definition of a physiological cross-sectional area (PCSA). The significance of this property lies in the fundamental fact that PCSA is directly proportional to the force generated in the muscle unit as it represents an area orthogonal to the fibers direction. Common sense tell us this area changes along muscle path and estimating its value might represent a difficult task. However, the PCSA can be estimated by capturing all the cross-sectional areas along the muscle length. Experimental anatomical studies have verified that a representative PCSA [63, 64] can be estimated using the total muscle volume and the fiber length applying the following expression:

$$PCSA = \frac{Muscle\ Volume}{Fiber\ Length} \tag{1}$$

Overall, muscle attachments, PCSA and muscle fiber length dictates the biomechanics of skeletal muscles since fiber length is proportional to muscle excursion while physiological cross-sectional area is proportional to maximum muscle force as seen in Figure 3-4.

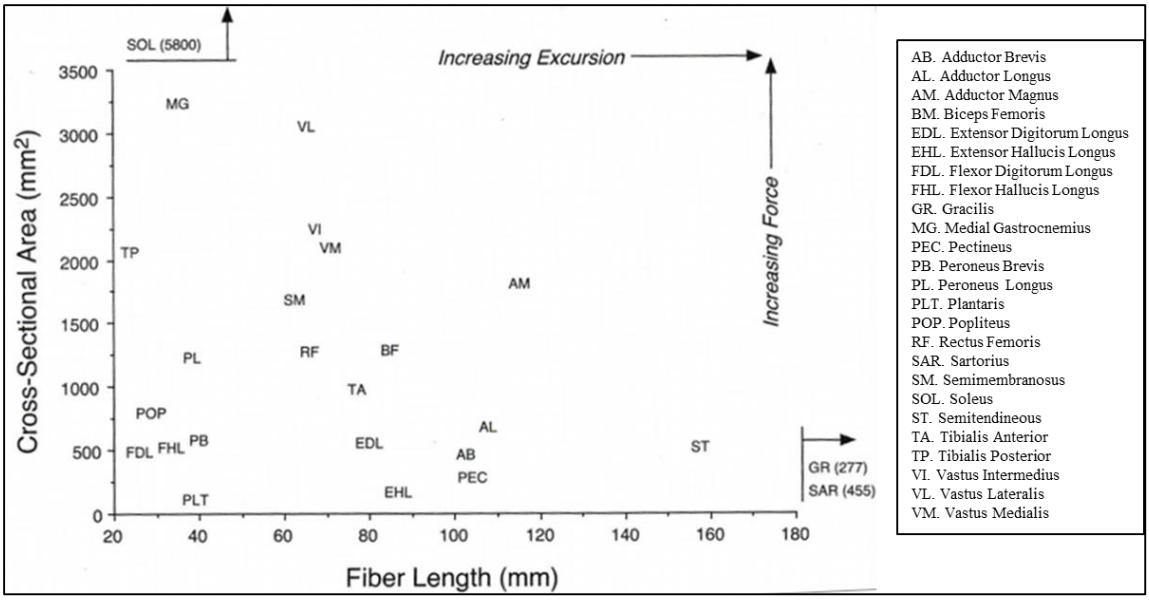

Figure 3-4: Lower Limb Muscles Fiber Length and Physiological Cross-Sectional Areas [65].

Muscle mechanics have been studied in vivo, in situ, and in vitro; but in most cases not all measurements needed could be obtained due to several limitations [66]. For instance, it is very difficult to maintain a muscle's biological life when they are isolated from the body for longs periods of time. In the past, extensive experimental work has been performed on frogs and toads mainly due to amphibians' characteristics, which allows to keep their mechanical properties for several hours when place in a physiological solution. It is also well known amphibian's muscle mechanical properties are similar to human muscles but at the same time similarities are limited. Therefore in order to validate similarities and dissimilarities of amphibian models, experiments on human muscles are needed. Engineers and scientists have also assumed muscles possess mechanical properties similar to common composite materials used in engineering applications. Using this unique approach, muscles could then be modeled as a fiber-reinforced composites [67] where muscle fibers are made of high tensile strength material and are embedded in another material called matrix. As explained before**,** adjoining connective tissues hold muscles together. Therefore the connective tissue could be considered the muscle matrix and the muscle fiber could be considered the fibers in the matrix.

To summarize, this section have provided a detailed grasp of skeletal muscle architecture-functionality and its relevance on the study of muscle mechanics at the microscopic and macroscopic level. The basic familiarity we have created until this point will allow us to link this knowledge to the next two sections where skeletal muscle path representation and mechanical models of skeletal muscles are discussed.

3.2 Skeletal Muscle Path Representation

To accurately quantify force and moment transmission in muscles, it is imperative to map paths that will properly represent lines of action. In addition, muscle path provides necessary information relevant to study of muscle mechanics such as muscle moment arm and muscle length. This section provides a comprehensive analysis of several methods which has been developed and used to generate muscle path representation. Namely, the straight-line representation, the centroid muscle representation, and the curved and wrapping muscle representation are presented in this section to understand the benefits, challenges, and limitations of each method. All the different approaches presented have been theoretically and experimentally validated for various musculoskeletal architectures. Additionally, implementation of these techniques should be based on muscle geometry and its anatomical landmarks. Once a muscle path has been established, muscle mechanical behavior could be modeled using kinematics and dynamic analysis.

3.2.1 Straight-line Skeletal Muscle Path Representation

This particular method allows to join the geometric centers of muscle attachments areas, namely the origin and insertion points, using a straight-line. The straight-line muscle path representation (SLMPR) allows for straightforward estimation of muscle moment arms and forces using classic methods of vector analysis [66]. The SLMPR is without a doubt the easiest way to model a muscle path but at the same time it has its limitations. There are specific sets of skeletal muscles where the straight-line approach can be implemented since some skeletal muscles may wrap around bones, diverging from a straight-line of action behavior. Dostal and Andrews [68] have stablished proper guidelines to accurately define skeletal muscles in the lower limb, where

the SLMPR can be successfully applied. Their experiment showed for several ranges of hip joint angles in the lower limb, various skeletal muscles can be modeled using the SLMPR. Their benchmark experiment modeled skeletal muscles as fixed elastic strings attached to their origin and insertion attachment points as seen in Figure 3-5. The interaction between strings with bones and/or other strings was then closely observed to determine valid ranges where the straight-line approach will yield to accurate force and moment estimation. Furthermore, this experiment reported three important outcomes: (1) it provided hip joint angles values where the SLMPR is valid, (2) it showed skeletal muscle SLMPR limits depend on hip joint angle, and (3) it presented skeletal muscles that should never be modeled using a SLMPR at any hip joint angle.

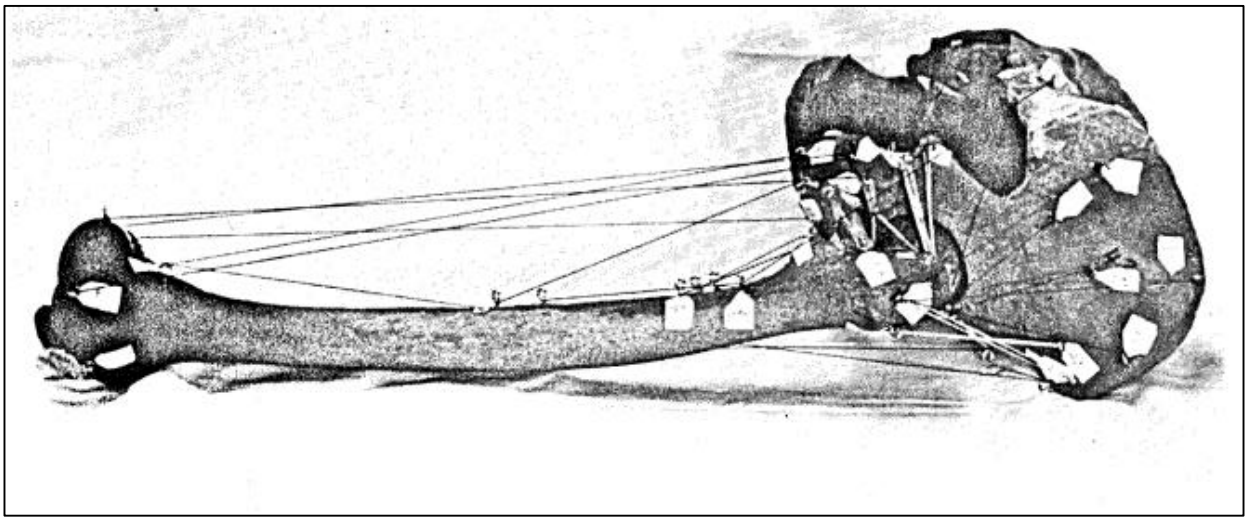

Figure 3-5: Hip Musculature Elastic Straight-Line String Model [68]

When applicable, the SLMPR has been used to predict how muscle arm moment, which is defined by the perpendicular distance from a joint center to its respective muscle line of action, varies relative to the shortest distance between the muscle line of action and the joint center. Figure 3-6 shows a geometric representation of the elbow joint of the brachialis (BRA) and the brachioradialis (BRD) where a triangle is formed by muscle's origin and insertion points and the

joint center (JC). The triangle formed by both the BRA and BRD clearly shows that the maximum value of moment arm (ma) is the shorter distance (D_s) between the joint center and a muscle's attachment points on the bone. Based on this simple two-dimensional model of the elbow joint, it has been proved theoretically and experimentally that a closed relation exists between the shortest attachment and muscle moment arm [69, 70].

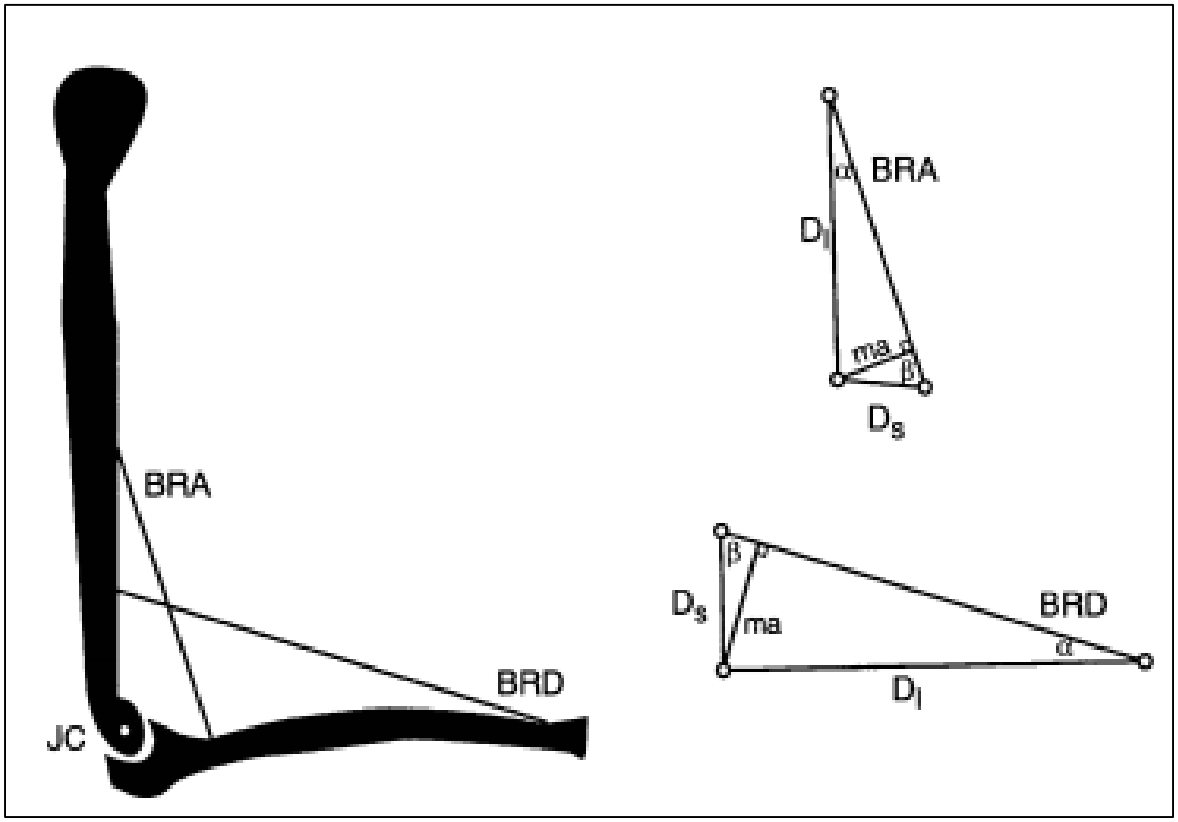

Figure 3-6: Two-Dimensional, Geometric Representation of Elbow Joint Using a SLMPR of the Brachialis (BRA) and the Brachioradialis (BRD) [69].

This study shows that muscle length on its own is not a good predictor for peak moment arm and instead D_s values and joint dimension should be used to properly quantify it. Furthermore D_s could be also used to properly normalize and scale available experimental muscle moments arm data obtained from different human specimens.

3.2.2 Centroid Model of Skeletal Muscle Path

Modeling skeletal muscles using a muscle centroid path provides a better geometrical representation of muscle's line of action but at the same time its implementation requires intrinsic parameters which are not easy to obtain. The method can be successfully implemented by arranging the centers of muscle cross-sectional areas, obtained from a number of segments along the muscle, to form a geometrical path. This procedure however requires cross-sectional information of muscles, which could be obtained from imaging or experimental procedures. The challenge is to use intervals small enough to accurately map the geometrical muscle line of action. As explained previously, the effective application of the centroid technique yields to a better representation of muscle's lines of action but it also comes with limitations. For instance once a path is mapped, the centroid muscle path represents a given muscle length, meaning a new centroid muscle path is defined by changes in muscle length or joint motion. Additionally, it is known that centroid muscle path representation neglects muscle pennation angle, which is a critical value needed to precisely quantify forces and moments of some muscles where pennation is relevant. Several experiments have been performed on skeletal muscles to tabulate muscle centroid data and to show numerical differences between the centroid path technique and the SLMPR [71]. Figure 3-7 shows experimental data obtained for the gluteus medius using the muscle centroid approach where it is visible, that for this particular muscle the SLMPR will not yield to accurate muscle force and moment quantification.

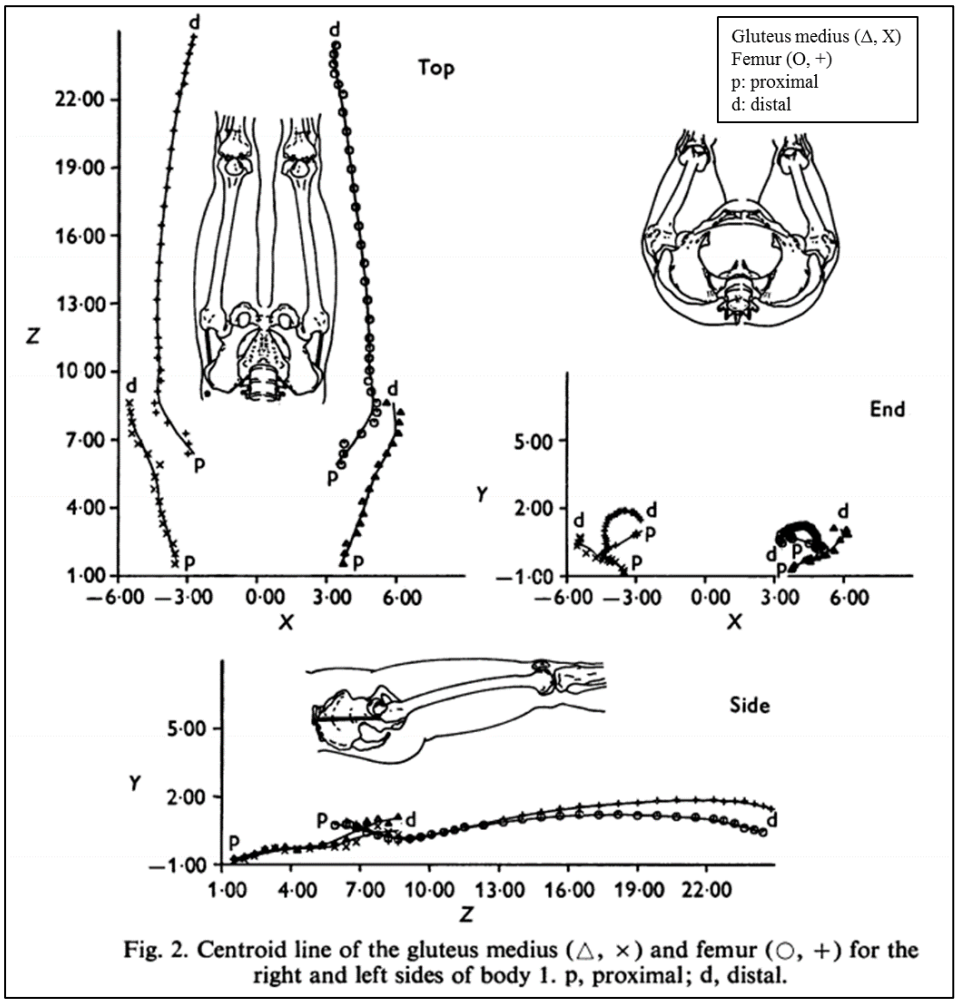

Fig. 2. Centroid line of the gluteus medius (△, ×) and femur (○, +) for the right and left sides of body 1. p, proximal; d, distal.

Figure 3-7: Centroid-Line Representation of Gluteus Medius and Femur [72]

3.2.3 Modeling of Curved and Wrapping Skeletal Muscles

Within the musculoskeletal system, there are muscles that are curved and muscles that wrap around anatomical constraints such as bones or other muscles as shown in Figure 3-8.

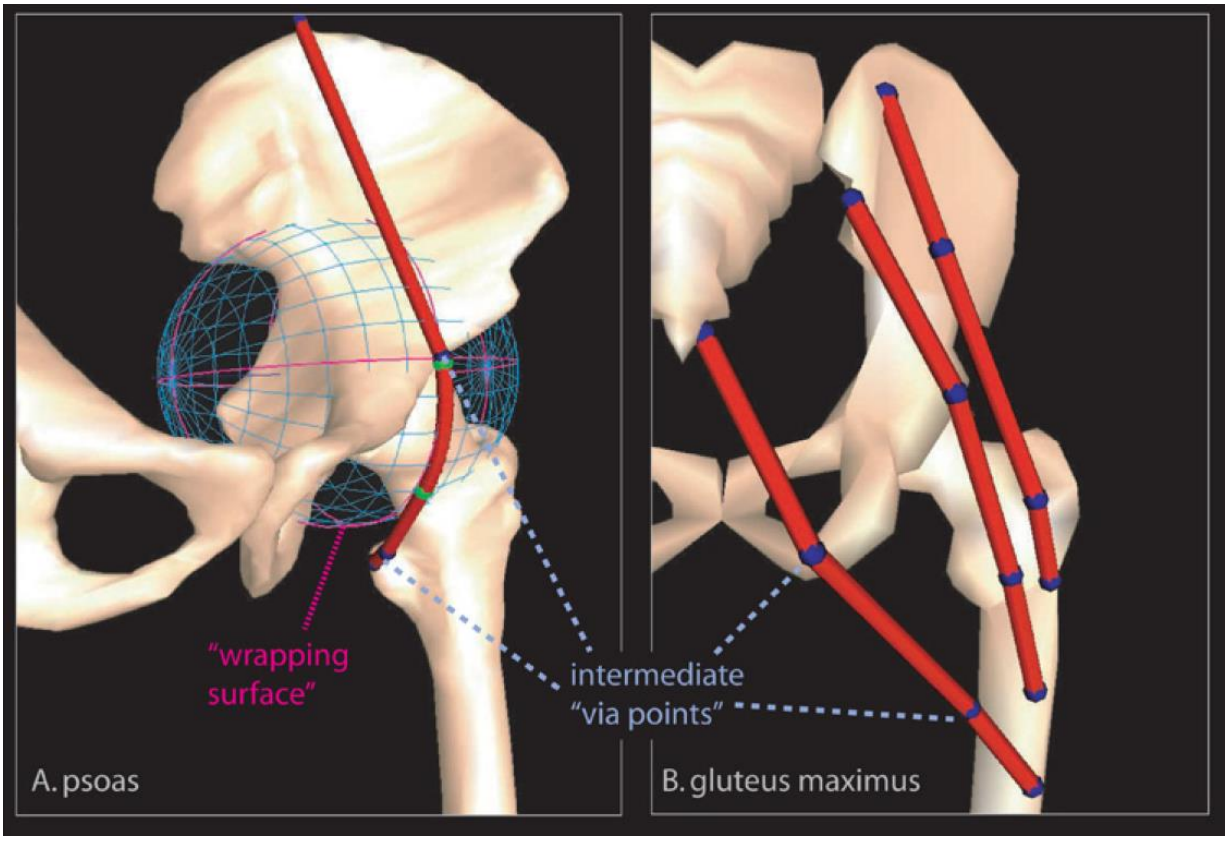

Figure 3-8: Psoas and Gluteus Maximus Muscle-Path Representation Using Curved Segments Wrapped Around Multiple Surfaces [73].

Similar to the centroid muscle path, curved muscle path representation requires additional parameters besides the standard required definition of origin and insertion points. Curved muscles could be accurately mapped by using straight-line or curve segments joined through a collection of specific geometrical data points. However, the modeling of the curve muscles' line of action is strenuous due to muscle length changes during concentric contraction. On the other hand, elucidating muscle wrapping is a challenging task as it adds the mechanical interaction of muscles with its surroundings. To account for muscle wrapping, simple one dimensional models have been

developed to define muscle line of action as it connects to the bone [74]. In addition, numerous novel mathematical methods and imaging techniques have been proposed and used to account for intricate muscle wrapping [54, 73, 75]. Particularly, these methods are computationally expensive and often call for optimization techniques [76] to improve the time required to refine wrapping objects. Once wrapping path has been established, the kinematics of wrapping muscle are easy to compute and could be resolved using classical kinematics theory. The dynamics, however, become laborious as muscle contact with other anatomical landmarks adds complexity to the mechanism. Thus, mechanical contact definition is of paramount importance to quantify muscle forces and moments. For instance, modeling friction becomes a critical constituent on muscle wrapping as it will considerably affect the dynamics of the problem. Modeling such contact constraints is not always a straightforward procedure since most of these physiological behavior have not been quantified mechanically.

3.3 Mechanical Modeling of Muscles

Once muscle paths are developed, muscle mechanical behavior can be analyzed using well known mechanical models such as the classic Hill's model [77]. Hill developed this lumped-parameter idealized force generator model based on experimental observations on isolated muscle fibers. His simplistic approach has remained as the standard technique to analyze muscle dynamics. The model uses three elements; a contractive element (CE), a series element (SE), and a passive element (PE) to estimate total muscle force generation (F^M) as shown in Figure 3-9.

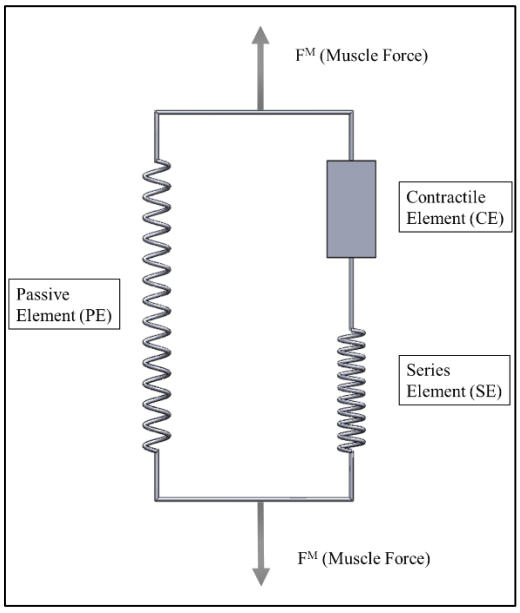

Figure 3-9: Hill-Type Muscle Model

The contractile element (CE) models muscle activation, mainly driven by forces developed at the sarcomere level during cross-bridge formation and is characterized by tension-length and force-velocity muscle behavior. The cross-bridge formation mechanism, which is the interaction between the actin and the myosin heads due to neuromuscular excitation, are beyond the scope of this dissertation and therefore not explained in detail on this chapter. However, vast information can be found in the literature describing the biomechanics of muscle contraction at the molecular level [65, 78-80]. Ultimately, the contractile element allows muscle shortening when activated and enables free shortening or lengthening when no activation is present.

In general, the series element (SE) models the compliance of tendons, aponeurosis, and myofilaments. This compliance enables rapid change of the muscle from an inactive to an active state. In addition, the SE acts as an energy storing mechanism. The properties of the SE yields to non-linear spring behavior and hence the spring representation in Hill's model. Considering the

nature of the series connection between the SE and CE, the shortening of the CE will always cause a stretch of the SE to keep the total muscle length. This particular scenario can be observed during isometric contraction.

The parallel element (PE) models the passive force exerted by connective tissue such as epimysium, perimysium, endomysium, and fascia. The PE is arranged in parallel with the SE and CE and similar to the SE, the PE's passive response exhibits non-linear behavior. When activation is not present and a muscle is stretched, the PE is exclusively responsible for the muscle passive behavior. Chapter 4 will reveal how this passive response is relevant to the study of developmental dysplasia of the hip.

Once the contribution of each the components in Hill's circuit has been estimated, total muscle force can be computed using the force exerted by each of the elements:

$$\begin{aligned} \boldsymbol{F^M} &= \boldsymbol{F_{PE}} + \boldsymbol{F_{SE}} \\ \boldsymbol{F_{CE}} &= +\boldsymbol{F_{SE}} \end{aligned} \tag{2}$$

The classic Hill model is controversial and there is vast discussion on the appropriate utilization of the circuit. Specifically, the literature has debated its limitations, simplicity, and complexity [81]. To this end, muscle models have been developed on a case basis where assumptions are adequate to represent muscle behavior and match experimental observations. Therefore, studies have been performed to yield modified Hill muscle models such as dimensionless lumped models and viscoelastic models [82-85]. Hill models have suggested that muscles generally develop two types of forces: active and passive. The contractile element contributes to muscle active tension, while the series element and the passive element contribute

to the muscle passive tension. Subsequently, for a fully activated muscle the tension-length will include a passive and an active component as shown in Figure 3-10.

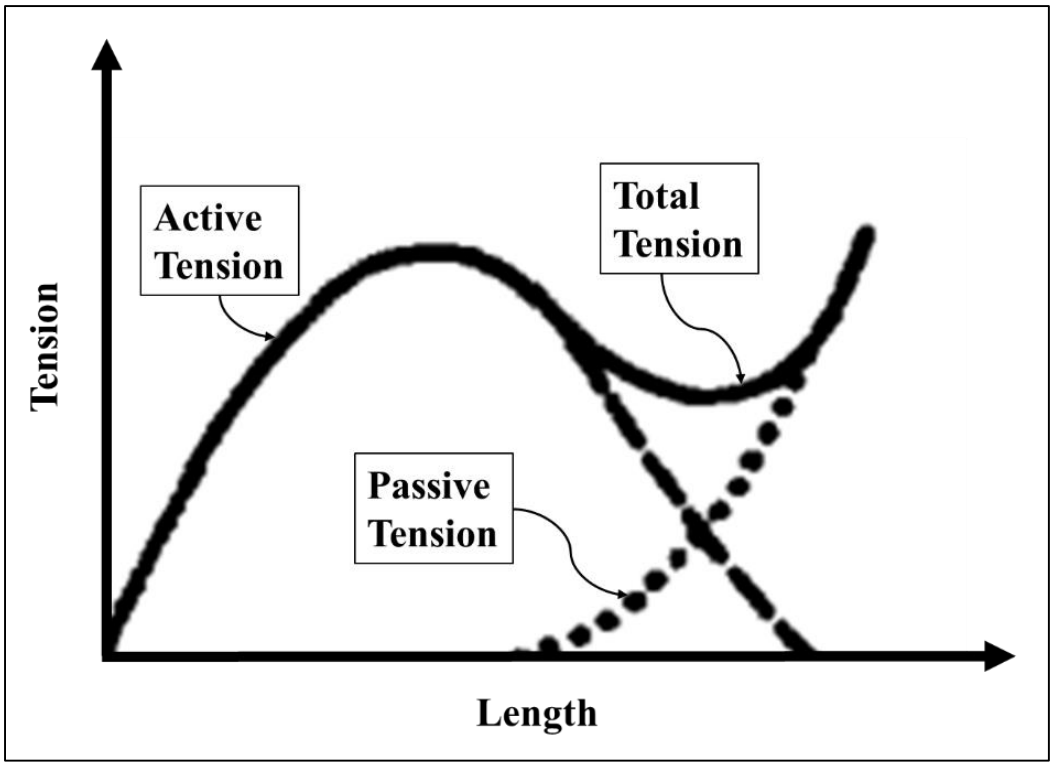

Figure 3-10: Muscle Tension-Length Curves Exhibiting Active and Passive Tension Behavior

3.3.1 Active Muscle Behavior

Muscle activation, which causes voluntary movement, represents a complex phenomenon. It all starts with a signal sent from the neuro-central system to skeletal muscles in order to achieve lengthening or shortening of muscles. As a rule of thumb, activation force generation decreases when shortening speed increases or vice versa. Thus, muscle tension during activation depends on two parameters: length and velocity. Analyzing force generation during regular contraction cycles represents a challenge due to the simultaneous changes of length and velocity. However, experimental studies have been performed under controlled conditions to analyze muscle active

tension at constant velocities and muscle active tension at constant lengths [65, 86]. Obviously, analyzing muscle activation using this approach represents unrealistic conditions but looking closely one can superposition both functions to develop a force relationship for length and velocity as seen in Figure 3-11. Although relevant for the study of muscle biomechanics, muscle activation is not utilized in the development of this dissertation and therefore is briefly explained in this section. Chapter 4 will reveal that hip reduction often occurs during relaxation, meaning passive muscle tension, besides gravity, is the sole mechanical force exerted in skeletal muscles.

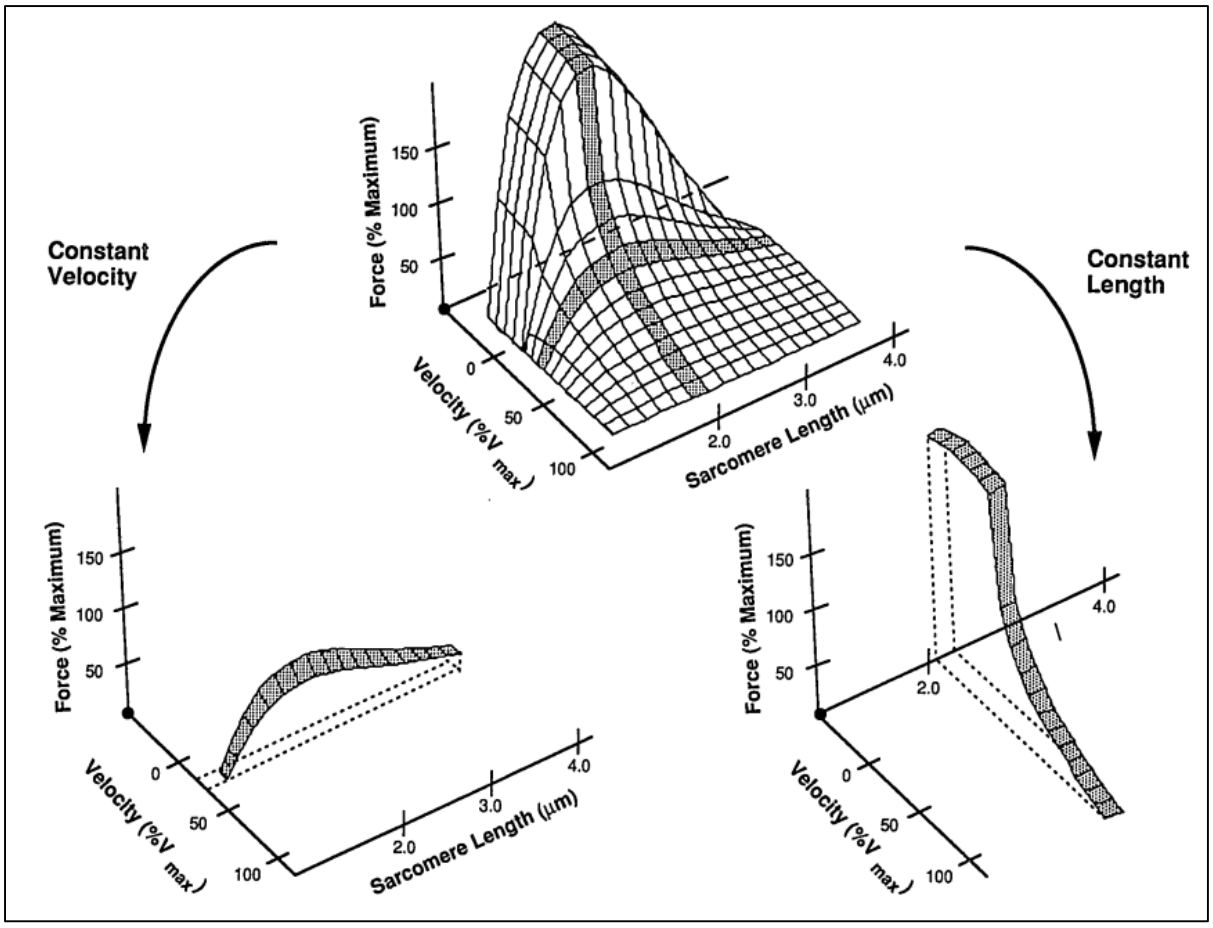

Figure 3-11: Generalized Relationship between Muscle Length, Force, and Velocity during Muscle Activation [86].

3.3.2 Passive muscle Behavior

When muscle activation is not present, skeletal muscle lengthening occurs mainly by the stretching of passive fibers. It is known that "when a relaxed skeletal muscle is stretched beyond its resting length, it behaves as a deformable body; that is, it deforms and provides passive resistance to the stretch. The resistance does not require metabolic energy and, hence, is called passive" [66]. Furthermore, Hill's model explicitly shows that the contractile element does not contribute to muscle forces developed in a passive state influenced mainly by the response of the series and the parallel elastic components [87, 88]. Research studies have suggested passive tension force is mainly due to connective tissue, namely the endomysium, the perimysium, and the epimysium but some authors suggests that most of the contribution might come from the myofibers [89] and some other studies have suggested passive tension contribution is due to stretching of the fascia [90].

Quantification of passive muscle response is critical to the study of both passive and active skeletal muscle behavior. Measuring activation forces directly from skeletal muscles represents a difficult task and has been attempted in the past without success. To overcome this obstacle, a straightforward and conservative approach has been suggested involving the use of total muscle force and passive force [91]. Such fundamental framework has been established using Equation (2) to estimate activation force contribution by subtracting total muscle force from passive force.

Passive muscle response has a soft tissue mechanical behavior similar to the found in all biological tissues. Furthermore, the physics underlining passive muscle response have shown its behavior does not obey Hooke's law and therefore muscle, and living soft tissue in general, will yield to non-linear deformations. Biological experimental numerical results [92, 93], as seen in

Figure 3-12, have shown that the relationship between the slope of the load-deflection curve and the load is more or less linear and can be described using the following linear relation:

$$\frac{dT}{d\lambda} = C_1 T + C_2 \tag{3}$$

where T is the passive force, λ is the stretch, and C_1 and C_2 are biological constants obtained from experimental data.

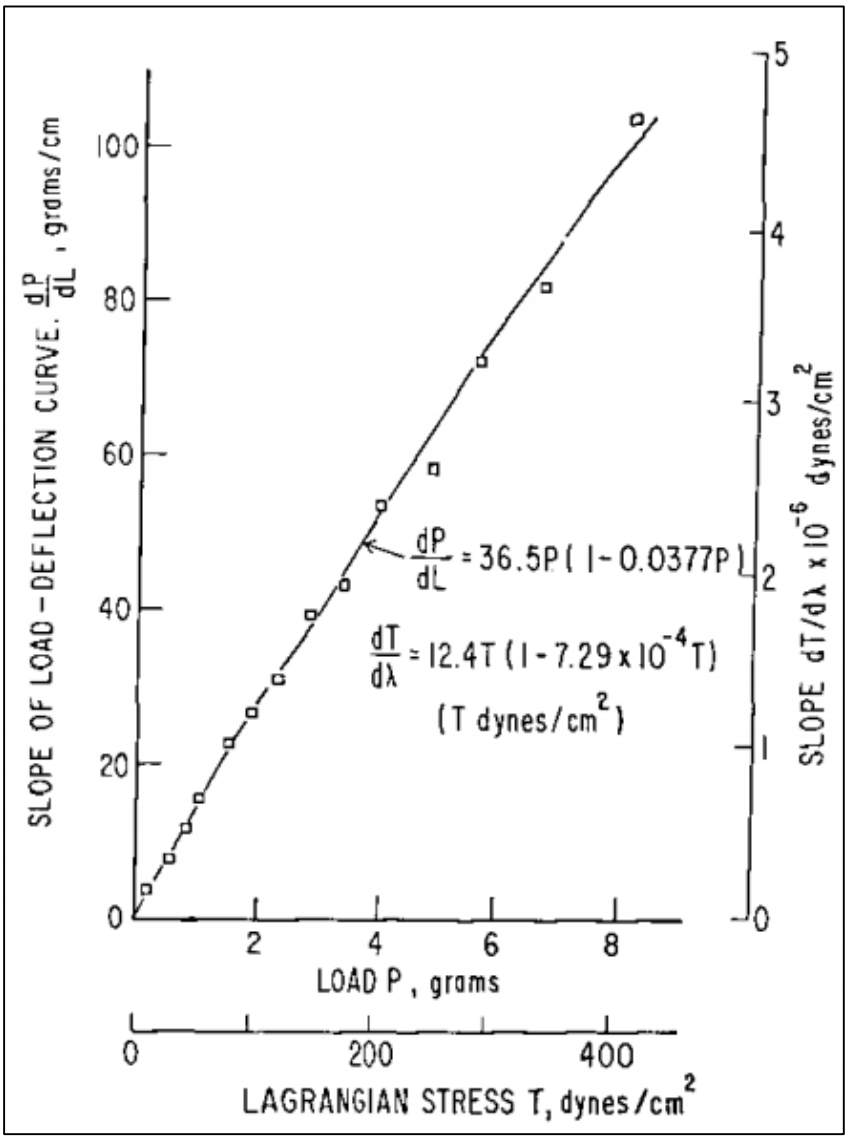

Figure 3-12: Fung's Biological Tissue Non-Linear Behavior [93].

Moreover Equation (3) can be integrated, using conservative boundary conditions, to yield a non-linear exponential relationship between the applied load and stretch:

$$T = \frac{C_2}{C_1}(e^{C_1(\lambda-1)} - 1) \tag{4}$$

Equation (4), describes the standard exponential relationship that has been commonly used to describe soft connective tissue mechanical behavior. For the purpose of this work the aforementioned relationship will be used to describe a musculo-tendon actuator driven by the responses of the parallel and the series elastic elements. The information provided in this chapter should be sufficient not only to understand the biomechanics of skeletal muscles but also to implement such models based on application. Chapter 4 will provide details and assumptions for accurate muscle modeling of the skeletal muscles in infants affected with developmental dysplasia of the hip.

CHAPTER 4: METHODOLOGY

The study of muscle mechanics is currently governed by biological experiments and mechanical models. While traditional approaches have used average and scaled anatomical data, it is important to recognize that one of the most important and challenging limitations of analyzing the human musculature, and the human body in general, is the fact that no individual has an identical anatomy. The kinematic and dynamics of locomotion strongly depends on mechanical interaction of the muscles with nearby bones, other muscles, and/or other connective tissues. Therefore, the most important task is to define morphometry and anatomical landmarks of bones and muscles accurately, which means there is a critical need to define the anatomical characteristics of muscles and bones, such as origins, insertions, and moment arms. For that purpose, a realistic model is needed to accurately investigate the biomechanics of the lower limb model. Additionally, it is known that developmental dysplasia of the hip is more common in females than males, with a female incidence of about ninety percent. Therefore, a ten-week old female infant was selected for the biomechanical studies on this dissertation. The three-dimensional model of the pelvis-femur-lower limb of the representative ten-week old female infant was generated based on the composite of CT-scans and MRIs of a six-month and a fourteen-year old female, as well as the Visible Human Project with the aid of anthropomorphic scaling of anatomical landmarks.

This chapter presents details of a successful patient-specific model reconstruction, which was used to investigate the forces and moments occurring on dislocated hips using the Pavlik harness. To that end, this chapter will introduce the following sections: section 4.1 will present the reconstruction of an idealized and representative patient-specific lower limb of a ten-week old

female infant; section 4.2 will explain how the reconstructed anatomy was assembled; section 4.3 will describe the implementation of passive muscle models in lower limbs; section 4.4 will provide a brief description of the Rigid Body Dynamics approach used to elucidate the kinematics and dynamics of lower limbs; section 4.5 will justify the use of a frictionless model on the hip joint; and section 4.6 will propose an innovative approach to calibrate the anatomical model to account for infant lower limb architecture.

4.1 Lower Limb Anatomical Reconstruction

The anatomical lower limb model was reconstructed using the aid of medical segmentation packages: Mimics and 3-matic (Materialise Inc., Plymouth, MI). The lower extremity was composed of the hip, femur, tibia, fibula, ankle, foot, and toe bones. It must be mentioned that symmetry was assumed along the sagittal plane, which divides the body into right and left portions (x-y plane). Thus only the right lower limb was modeled.

Due to the presence of large cartilaginous zones, the MRIs and CT-scans of a neonate offer a challenge in the reconstruction of the complete anatomy based on medical segmentation software alone. Moreover, retrospective MRIs and CT-scans of a subject with developmental dysplasia of the hip focus mainly on the hip region, and therefore, do not provide the required geometric information of the rest of the anatomy. As such, a model was constructed from the composite of Ct-scans of a six-month and fourteen-year old female, as well as the Visible Human Project with the aid of anthropomorphic scaling of anatomical landmarks in order to assemble the ten-week old infant model. It is also well-known that bone growth is not proportional in all directions [94], thus, anisotropic parameters were used for all of the lower limb bones.

For hip reconstruction, the starting point was to obtain rough bone geometry contours from CT-scans of a six-month old female infant and then superimpose it on well-defined bone geometry obtained from high quality CT-scan data of a fourteen-year old female [95]. Both the six-month old female infant and the fourteen-year old female were superimposed so the iliac spines and acetabuli were aligned as shown in Figure 4-1.

Computational frameworks for simulating muscle mechanics are currently available [96-98], but unfortunately, hip dislocations cannot be simulated using these commercial and research packages.

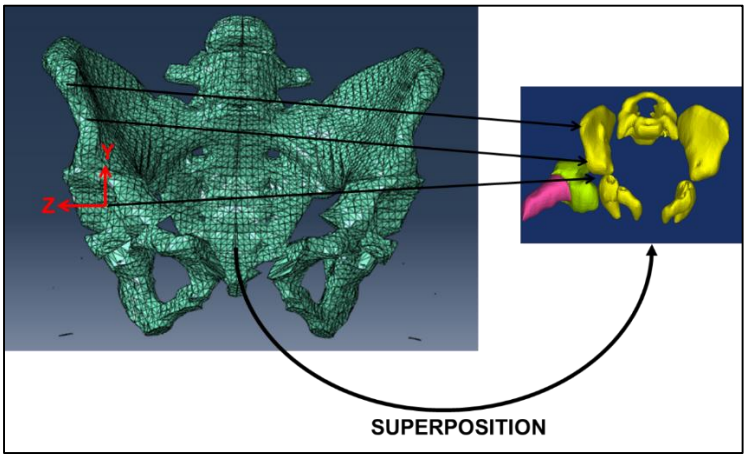

Figure 4-1: Superposition of a Reconstructed Model of a Fourteen-Year Old Female (left) with a model Rendered From CT-scans of a Six-Month Old Female Infant [95].

In addition, the superposition technique accounted for the hip widening that occurs in females during puberty. After successful reconstruction, the model of the six-month old female infant was scaled to that of a ten-week old female infant by the matching infant orthopedic data found in Hensinger's Standards in Pediatric Orthopedics [99]. The final pelvic anisotropic scaling factors were determined to be: 0.35 in the x-direction, 0.3 in the y-direction, and 0.35 in the z-direction. The following final measurements were reported for the acetabulum: acetabulum depth

was approximately 7.9 mm; acetabular depth-width ratio (ADR) was 45%; and acetabulum diameter was approximately 17.5 mm.

High-quality Ct-scans and MRIs from the Visible Human Project [100] were used to reconstruct the femur, tibia, fibula, ankle, foot, and toe bones. The geometry was reconstructed using the superposition approach used for the pelvis. Scaling parameters for all the other bones of the lower extremity were found to be: 0.23 in the x-direction, 0.22 in the y-direction, and 0.25 in the z-direction. The femoral head had a diameter of 14 mm and was assumed to be perfectly spherical as observed during the infant dissection shown in Figure 4-2.

Figure 4-2: Spherical Head in Neonates: Computational Model (Left) and Dissection (Right).

The femoral anteversion angle also plays a critical role on hip reduction since it will affect muscle force and moment contribution while the Pavlik Harness is in use. This particular angle defines the difference between the axis of the femoral neck and the transchondylar axis of the knee as explained in chapter 2. This angle ranges typically from 30° to 40°, but can reach up to 100° as seen in Figure 4-3.

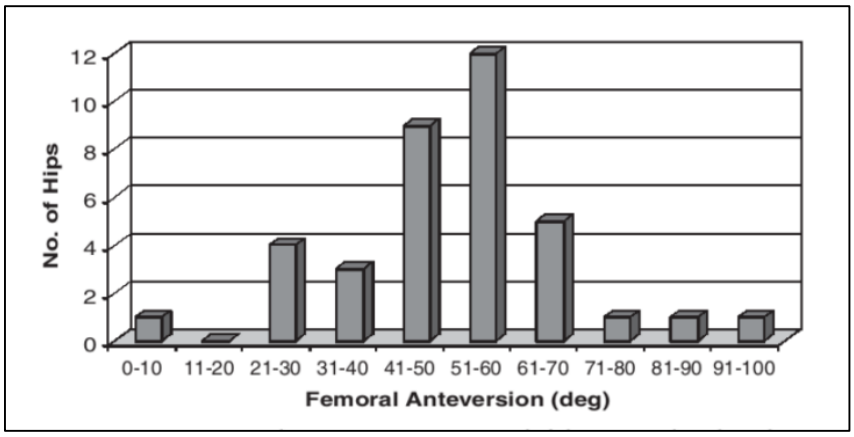

Figure 4-3: Femoral Anteversion in Children with Developmental Dysplasia of the Hip [101].

The anteversion angle decreases in adulthood to about 15°. It has been shown that anteversion angles between 0° and 40° has relatively small effect on the isometric moment-generating capacity [102]. For the main study a representative average anteversion angle of 50° [101] as seen in Figure 4-4. Although the main study was performed on the case exhibiting a femoral anteversion angle of 50°, an analysis over a range of angles was also performed for calibration purposes. Lower limb models with anteversion angles of 20, 30, 40, 60, and 70 were selected aiming to compare forces exerted during model calibration.

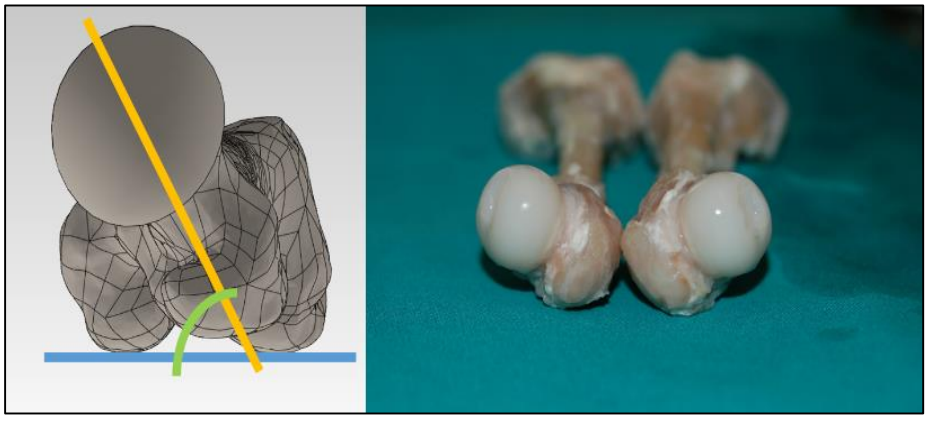

Figure 4-4: Illustration of 50° Anteversion Angle in 3D Computational Model (Left) and a Dissected Femur Showing Anteversion Angle (Right).

4.2 Lower Limb Anatomical Assembly

After anatomic reconstruction of the lower limbs. Solidworks was used to assemble all components as seen in Figure 4-5. To assemble the femur to the pelvis origins and orientations in both bones were specified as defined in the literature [68].

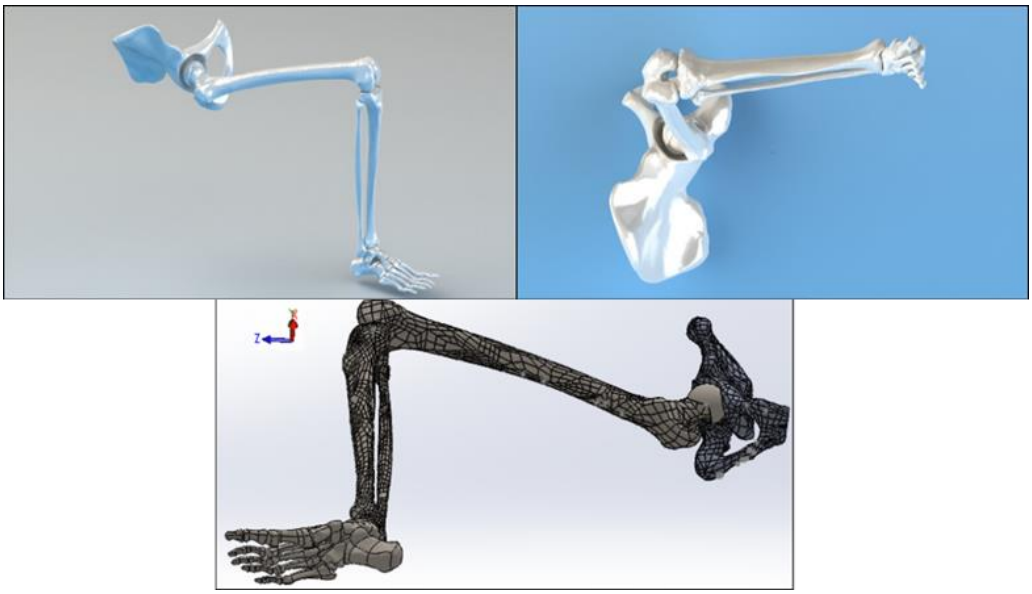

Figure 4-5: Reconstructed Lower Limb of 10-Week Old Female Infant.

The origin of the inertial Cartesian reference frame was located at the center of the acetabulum for the hip and at the center of the femoral head for the femur. Five adductor muscles were identified as mediating muscles during close reductions: (1) Pectineus, (2) Adductor Brevis, (3) Adductor Longus, (4) Adductor Magnus, and (5) Gracilis. The Adductor Magnus is a large triangular muscle with extensive femoral insertion; consequently, it is commonly represented by three effective components: (a) Adductor Magnus Minimus, (b) Adductor Magnus Middle, and (c) Adductor Magnus Posterior. Origin and insertion points were defined using the anisotropic scaling parameters previously mentioned on coordinate points obtained in experiments by Dostal and Andrews on the lower extremity as seen in Figure 4-6. For this study, musculoskeletal tissue is

modeled using a straight-line muscle path representation since lines of action do not intersect in the range of motion of interest, allowing to use classical methods of vector analysis [68].

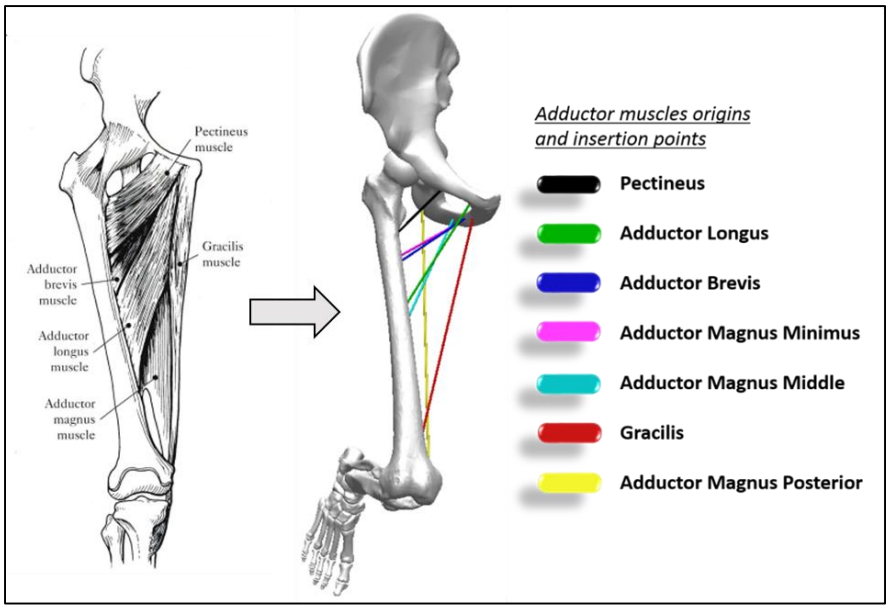

Figure 4-6: Anterior View of Adductor Muscles Origin and Insertion Points [103].

Once the model was assembled, the hip was able to be computationally dislocated to match physiological dislocations according to the dislocation grade under investigation as seen in Figure 4-7.

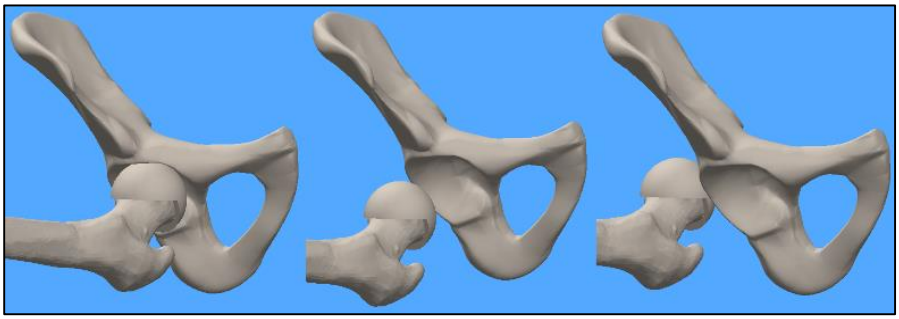

Figure 4-7: Hip Dislocation: Healthy Hip (Left), Grade 3 (Center), and Grade 4 (Right).

To account for proper weight distribution of muscles attached to the lower limbs, calculations of the total body mass were based on a ten-week old female infant at the 50th length-

for-age percentile [104] as seen in Table 4-1. Centers of mass were also determined, thus achieving accurate load and moment distribution in the model [105]. Gravity acts as the sole external driving load in the dynamics model to be described later. Moreover, the constraints assigned to the three-dimensional model serve to restrain the motion within the envelope realized with the Pavlik harness during Grade 1-4 studies to constraint the knees in a hyperflexed configuration for Grade 4 studies.

Table 4-1: Lower Extremity Mass Distribution.

Total Body Mass (BM):	**7.26 kg**	
Limb	%BM	Mass (kg)
Thigh	9.45	0.69
Leg	4.2	0.30
Foot	1.35	0.10
Full leg	1.5	1.09

4.3 Lower Limb Skeletal Muscle Modeling

To model the response of lower limbs muscles, proper assumptions are needed to effectively elucidate the biomechanics of developmental dysplasia of the hip. Chapters 2 and 3 laid the foundations needed for understanding of developmental dysplasia of the hip biomechanics and this section will use the background information previously presented to develop a realistic muscle model for the adductors. It has been documented that reductions of developmental dysplasia of the hip with the Pavlik harness occur passively with muscle relaxation in deep sleep [106, 107]. In recent clinical studies, sleep was induced to attain muscle relaxation, and, in flexion and abduction, towels adjusted to the appropriate height were placed under the knees to avoid

forcible abduction and it was clinically observed that under mild sedation and in natural abduction and flexion, the spontaneous reduction with the Pavlik harness is reproduced [108]. This study in particular further justifies the passive muscle model to be developed in this section. Chapter 3 revealed that skeletal muscles in general produce two kind of forces, active and passive, which sum to compose muscle total force. The active component is due to the contraction of muscle fibers that generate force and bear load, while passive components are due to stretching of muscle fibers, the basal lamina, and the muscle fascia [109]. As previously explained, without the presence of neuromuscular activation, muscle fibers and tendons are often considered mechanically in series in skeletal muscle and its structural arrangement will yield similar forces in both. It is important to acknowledge muscles and tendons, as well as connective tissue in general, display time-dependent behavior. Thus connective tissue will present viscoelastic behavior and should be analyzed with this concept in mind. Moreover, passive response is characterized as hyperelastic.

Chapter 3 presented well-known passive models [110, 111], which are extensively used for biological soft connective tissue based on the experimental observation that such passive tissue exhibits a fairly linear relationship between the stiffness and muscle stretch leading to an exponential behavior of the force-stretch curve. A novel Hill-based model [82, 84] had been proposed to estimate passive muscle force by normalizing it using a peak isometric muscle force as shown in Equation (5):

$$\overline{F^{PE}} = \frac{F}{F_o^M} \tag{5}$$

where is F^{PE} the normalized passive muscle force, F_o^M is the peak isometric muscle force, F and is the total muscle force. It is also been reported that peak isometric force is proportional to its physiologic cross-sectional area (PCSA) as seen in Equation (6):

$$F_o^M = C\ (PCSA) \tag{6}$$

where C is a biological constant and has a value of 25 N/cm^2 [84] and was estimated to scale physiologic cross-sectional areas that were measured in young adult cadavers to match moment curves measured on young subjects. Furthermore, it has been reported [112] that F^{PE} can be expressed as:

$$\overline{F^{PE}} = \frac{e^{K^{PE}(\lambda-1)/\varepsilon_o^M} - 1}{e^{K^{PE}} - 1} \tag{7}$$

where K^{PE} is an exponential shape factor with a value of 4.0 obtained from OpenSim (National Center for Simulation in Rehabilitation Research, Palo Alto, CA) [96], ε_o^M is the passive muscle strain with a value of 0.60 for young adults, and λ is the optimal muscle-fiber length (stretch). Moreover, the stretch can be written as $\lambda = L/L_o$ with L being the deformed length, and $L_o$being the initial muscle length at rest, measured at 20° abduction and 120° flexion for newborns. This flexion and adduction 'neutral' configuration accounts for the fact newborns maintain a posture similar to the fetal positioning for the first few months after birth with the hips flexed in toward the belly and wide apart. This initial muscle length at rest is also multiplied by a specified muscle pre-stretch for the lower extremity muscles and its value is usually between 20-30%. By combining Equations (5), (6), and (7), an expression can then be derived to obtain passive muscle force as function of stretch as seen in Equation (8).

$$F = PCSA\left[a\left(e^{b(\lambda-1)} - 1\right)\right] \qquad \begin{cases} a = \dfrac{C}{e^{K^{PE}} - 1} = 0.466\dfrac{N}{cm^2} \\ b = \dfrac{K^{PE}}{\varepsilon_o^M} = 6.667 \end{cases} \tag{8}$$

To estimate physiologic cross sectional areas (PCSA), MRI data for the adductor brevis of a ten-week old month female was used. A PCSA of 0.41 cm^2 was computed by measuring the volume of the adductor brevis and dividing it by its average length. A shape factor was then defined as the ratio between an adult PCSA and the ten-week old female infant PCSA by using a PCSA of 11.52 cm^2 of an adult's adductor brevis [113]. The adductor brevis shape factor of 0.0036 was then used to scale experimentally measured physiologic cross-sectional areas of the rest of the adductors.

Table 4-2: Scaled Ten-Week Old Female Infant Physiologic Cross-Sectional Areas Using Adductor Brevis Shape Factor [113].

f = 0.036	**Friederich PCSA (cm^2)**	**TWOFI scaled PCSA (cm^2)**
Pectineus	9.03	0.321
Adductor Brevis	11.52	0.410
Adductor Longus	22.73	0.809
Adductor Magnus Minimus	25.52	0.908
Adductor Magnus Middle	18.35	0.653
Adductor Magnus Posterior	16.95	0.603
Gracilis	3.73	0.133

4.4 Lower Limb Rigid Body Dynamics Model

To elucidate the biomechanics of developmental dysplasia of the hip, a rigid-body dynamics model was used. Thus, the lower limbs bones were assigned a rigid-body behavior. Such assumption is proven to be valid since muscle forces developed in infants, especially under passive tension, do not contribute significantly to their elastic deformation. On the contrary, muscle

response is relevant and its behavior is modeled using the straight-line approach explained in Chapter 3. Moreover, its viscoelasticity and non-linearity are accounted for in the exponential model previously presented.

Numerical rigid body dynamics was carried out using the ADAMS dynamics motion analysis in Solidworks. The governing differential equations of motion provided in Equation (9) :

$$\underline{\underline{M}}\,\underline{\ddot{q}} + \beta\underline{\phi}_q^T - \underline{\underline{A}}^T\underline{F}\left(\underline{q}, \underline{\dot{q}}\right) = 0 \tag{9}$$

are numerically solved subject to the natural constraints $\underline{\phi}\left(\underline{q}, t\right) = 0$. The system mass matrix is $\underline{\underline{M}}$, the vector of generalized coordinates for the displacements is $\underline{q}$, the Lagrange multiplier adjoining the gradient constraints $\underline{\phi}_q$ is β, the set of configuration and applied motion constraints is denoted by $\underline{\phi}$, the matrix $\underline{\underline{A}}^T$ projects the applied force in the $\underline{q}$ direction, and $\underline{F}$ is the vector of applied forces. The governing equations of dynamics described in Equation (9) are Newton's laws of motion augmented via a Lagrange multiplier by constraints. The force vector $\underline{F}$ is in general a function of displacement, linear in the case of a Hookean solid or non-linear as in our case as in Equation (9), and a function of the time-derivative of the displacements in case of the presence of damping. In this study, the Gear Stiff (GSTIFF) integrator was used, the Jacobian was updated at each time-step, 25 sub-level iterations were taken per time-step, and the initial, minimum, and maximum integrator step sizes were set to 1 x 10^{-4}, 1 x 10^{-7}, and 1 x 10^{-2} respectively. Custom functions were written in Solidworks for each of the muscles studied using the model described in Equation (8) with their respective physiologic cross-sectional areas.

4.5 Hip Joint Lubrication

Physiologically, the hip joint is considered a synovial joint on which the bone ends are covered by a slippery tissue called articular cartilage. Such joint bears diverse mechanical loads during physical activities. Depending on activity, forces exerted in the hip joint can be modest or large in magnitude. In humans, these actions can go from standing or sleeping to strenuous motions such as running or jumping. Thanks to the complex lubrication mechanism in the hip joint, the articular cartilage presents little wear regardless of physical activity and intensity under normal circumstances. Such mechanism acts under low coefficients of friction, which for the articular cartilage can vary from 0.002 to 0.04 [114]. These values can be then compared to common engineering materials, as seen on Table 4-3, to develop an understanding of their impact in the infant hip joint model.

Table 4-3: Friction Coefficients for Common Engineering Materials.

Materials		**Friction Coefficient**
Articular Cartilage	Cartilage, Tissue, Bones	0.002 - 0.04
Ice (0°C)	Ice (0° C)	0.01 – 0.1
Diamond	Diamond	0.1
Wood	Wood	0.25 - 0.5
Steel	Steel	0.8
Glass	Glass	0.9 - 1.0
Rubber	Rubber	1.16
Silver	Silver	1.4

Ultimately, the hip joint in the ten-week old female infant can be modeled mechanically as a multi-axial ball and socket that creates a frictionless bearing point as shown in Figure 4-8. Moreover, for the present analysis the contact between surfaces was assumed to be frictionless using a restitution coefficient of zero.

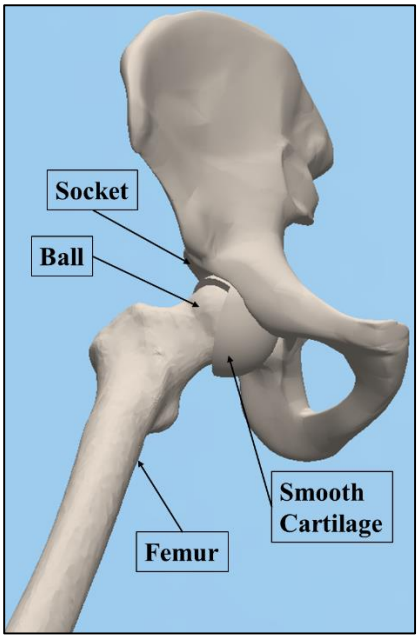

Figure 4-8: Ball and Socket Hip Joint Frictionless Model.

4.6 Lower Limb Calibration Model

Since the passive muscle model previously developed was specifically based on a young adult, the constants ***a*** and ***b*** in Equation (9) needed to be recalibrated for a ten-week old female infant and also to stiffen the exponential function to account for ligaments that start acting at the limit of ranges of motion, namely, the iliofemoral, pubofemoral and ischiofemoral ligaments which help to stabilize the hip joint. The muscle model was calibrated by calculating the factors that allowed to precisely replicate the clinical observation that equilibrium is attained when infants are

supine and the hips are placed in abduction at 80° and 90° flexion. That is, in this position, the passive action of the muscles holds the legs in place. Constants ***a*** and ***b*** were tuned in this model until the equilibrium configuration was achieved by only using muscle passive tensions. For the model with a femoral anteversion angle of 50°, constant ***a*** was found to be 0.0337 N/cm^2 and ***b*** was found to be 13.95. It is important to mention that there is no unique set of values for ***a*** and ***b***. However there is a minimum value requirement for ***b***, which is needed to stiffen the curve in order to achieve physically realistic equilibrium at 80° abduction. The constants ***a*** and ***b*** are inversely related; while ***b*** needs a minimum value to allow the model to achieve realistic muscle behavior, ***a***, which is used to find final equilibrium, is found through iteration once ***b*** has been established. The passive muscle force behavior for our calibrated ten-week old female infant model is presented in Figure 4-9 where it observed that the exponential behavior becomes very pronounced after a lambda (λ) value of about 1.35.

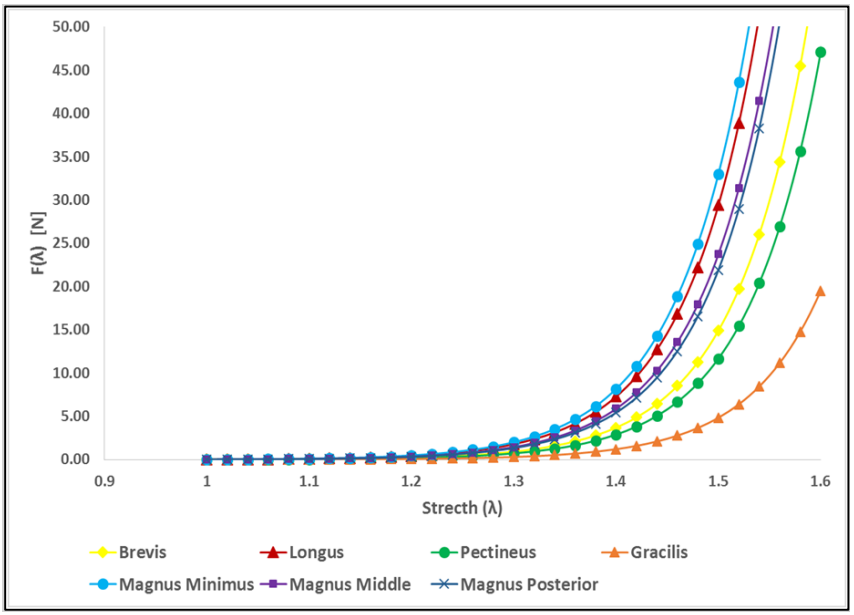

Figure 4-9: Ten-Week Old Female Infant Passive Force versus Stretch for Calibrated Model.

The equilibrium model stiffens significantly after this value due to the previously mentioned hip joints ligaments that prevent any further abduction of the legs past an angle of 80°. Figure 4-10 also shows a comparison of the force-stretch behavior between the ten-week old female infant calibrated model and the young adult of the adductor brevis where it is clearly seen our calibrated model stiffens faster once it get close to the limits of ranges of motion as expected. After a close comparison between all the adductor muscles, it is found that all muscles display the same behavior as the brevis.

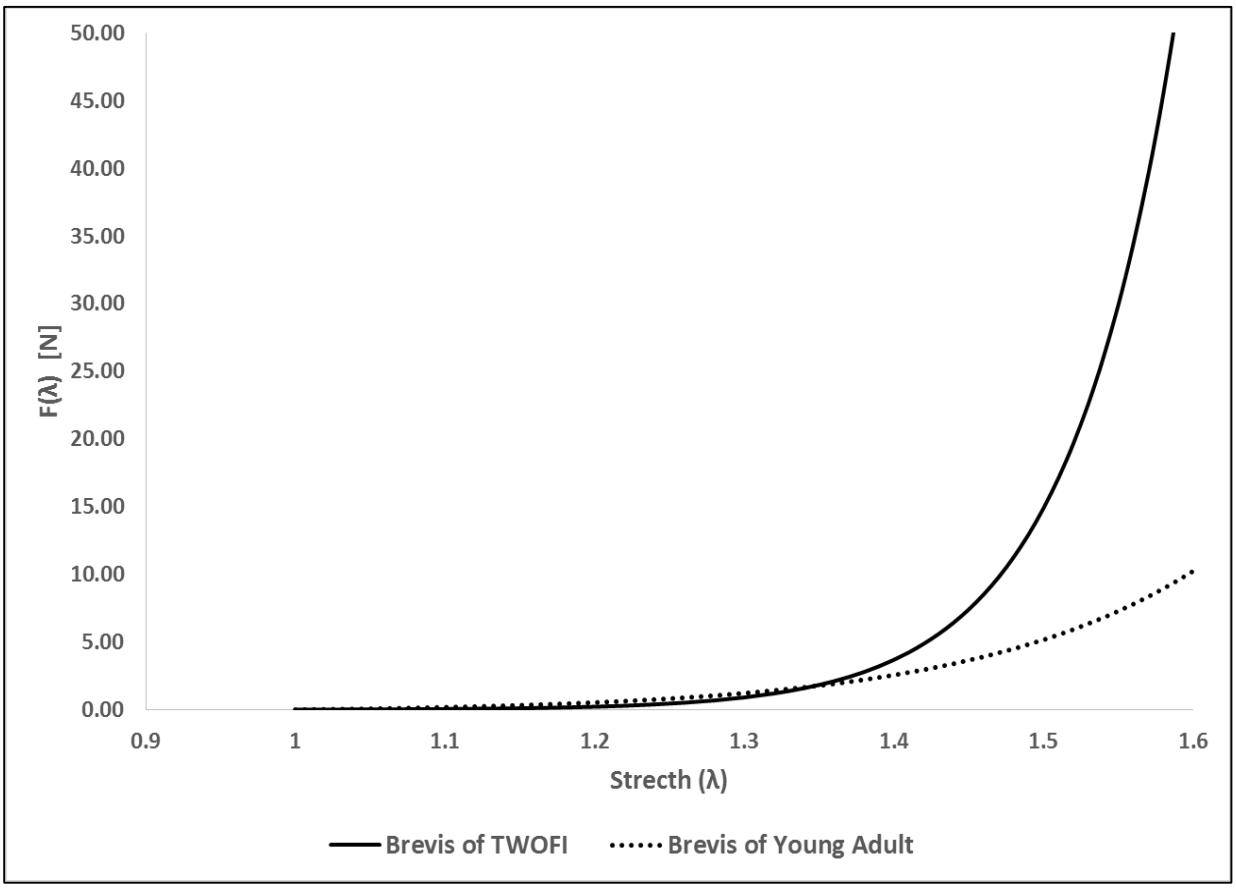

Figure 4-10: Adductor Brevis Force-Stretch Comparison between Ten-Week Old Female Infant and Young Adult Model.

Figure 4-11 provides the x-y and x-z views at equilibrium with reaction force(s) imparted at the contact(s) of the femoral head and the acetabulum shown as single headed (yellow) arrows whose magnitude is proportional to the size of the arrow. Muscle force and moment contribution at equilibrium clearly show that the Pectineus and the Adductor Brevis are the main muscle contributors.

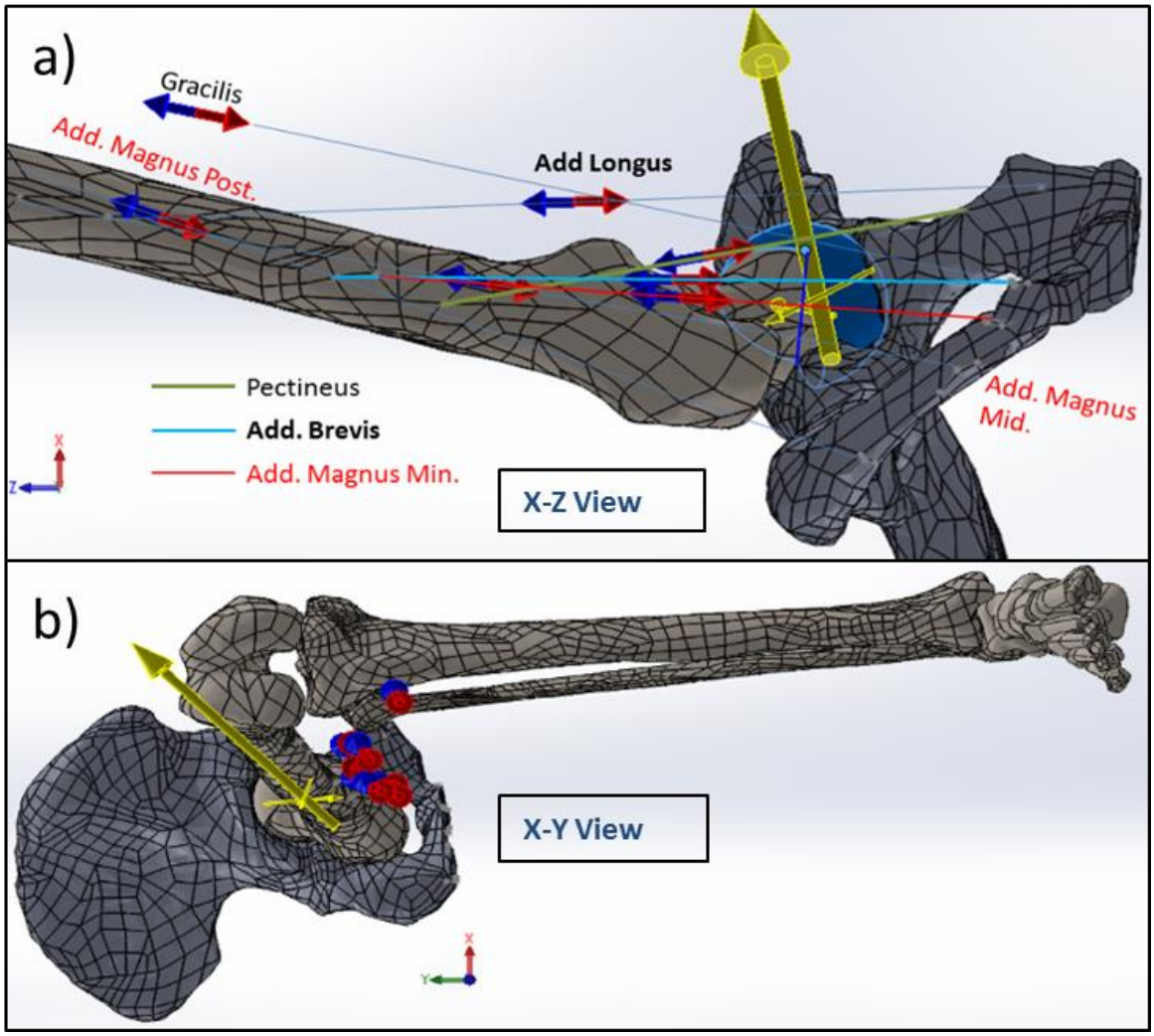

Figure 4-11: Calibrated Model: a) Contact Forces (Single Headed Arrow) and Muscle Lines of Action (Double Headed Arrow) on XZ-Plane, b) Contact Force (Single Headed Arrow) and Muscle Lines of Action (Double Headed Arrow) on XY-Plane.

Table 4-4: Muscle Force and Moment Contribution at Equilibrium Configuration.

	λ (Stretch)	Total Force (N)	X-Moment (Nm)	Y-Moment (Nm)	Z-Moment (Nm)
Pectineus	1.710	45.84	0.2834	0.3328	0.0738
Adductor Brevis	1.523	15.01	0.1353	0.1342	-0.0165
Adductor Longus	1.422	1.35	0.0138	0.0028	-0.0006
Adductor Magnus Minimus	1.392	1.83	0.0189	0.0013	-0.0014
Adductor Magnus Middle	1.316	0.84	0.0085	-0.0013	-0.0012
Adductor Magnus Posterior	1.229	0.33	0.0031	-0.0030	-0.0007
Gracilis	1.357	0.33	0.0040	0.0016	-0.0010

CHAPTER 5: RESULTS

The lower extremity model of the ten-week old female infant was used to quantify force and moment generation of the adductor muscles. It is known from clinical observation that reduction is successful whenever the Pavlik harness is used on Grade 1 and Grade 2 dislocations [40], thus these two grades were analyzed but values are not reported. For this dissertation the grade classification established by the International Hip Dysplasia Institute [36] was adopted to characterize dislocations of developmental dysplasia of the hip since it is in general applicable to infants and to older children as explained in Chapter 2. The ten-week old female infant model was dislocated as previously explained to investigate dislocation Grades 1-4. Subtle dislocations are modeled for Grades 1 and 2 as described by the International Hip Dysplasia Institute as seen in Figure 5-1a and Figure 5-1b.

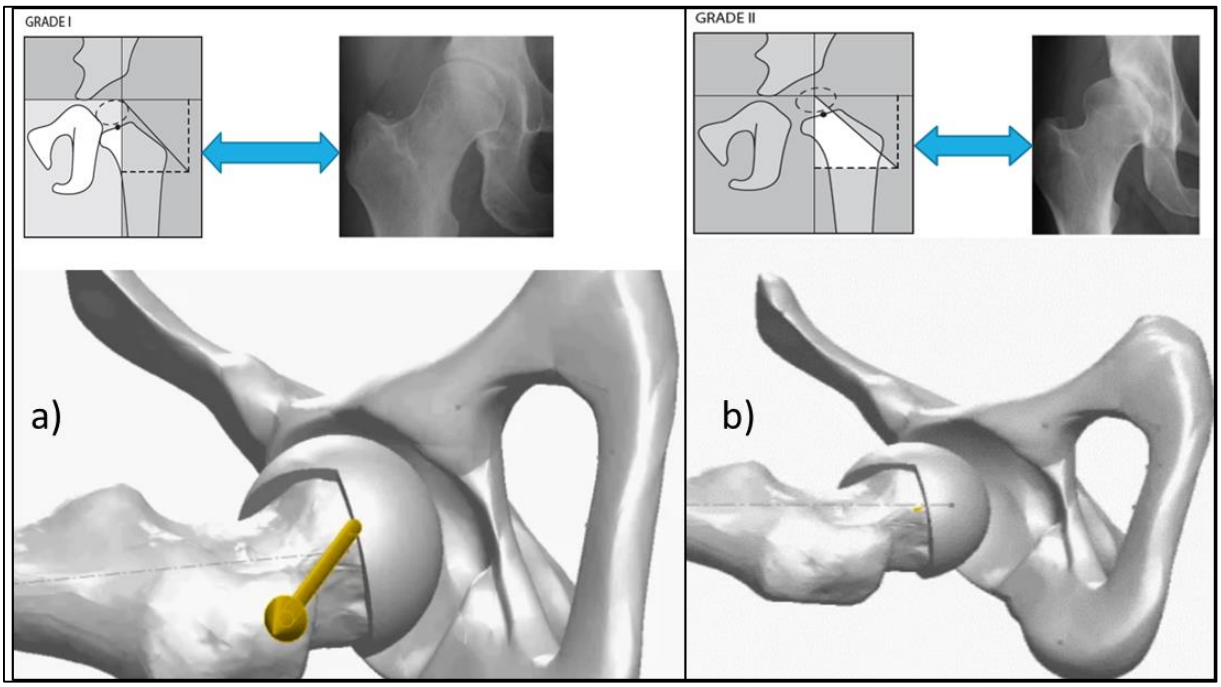

Figure 5-1: a) Grade 1 and b) Grade 2 Anatomical dislocations.

Force and moment contribution of the adductor muscles while the Pavlik harness is being used are reported for Grade 3 and Grade 4. Results provided insight of their contribution to reduction of developmental dysplasia of the hip on severe Grade 3 and Grade 4 dislocations whenever the Pavlik harness is used and gravity is acting.

5.1 Grade 3 Dislocation Results

For Grade 3, the ossification center is at the level of the superolateral margin of the acetabulum. The femoral head was placed at the rim of the acetabulum as seen in Figure 5-2 , and the center of the femoral head was placed at x = -3.44 mm, y = 1.14 mm, z = 6.59 mm relative to the origin located at the center of the acetabulum. Table 5-1 provides force and moment contributions of the adductor muscles while the Pavlik harness is being used.

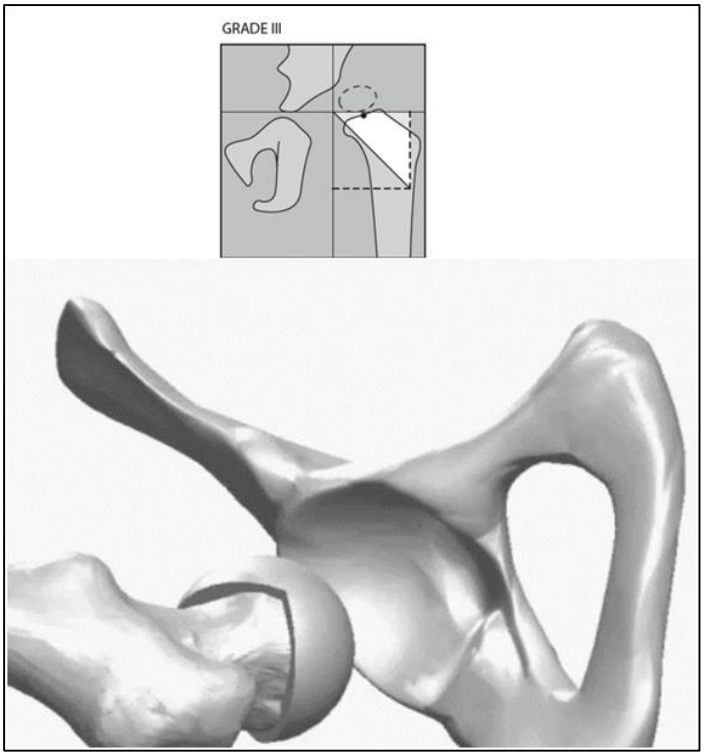

Figure 5-2: Grade 3 Anatomical Dislocation.

Table 5-1: Muscle Force and Moment Contribution on Grade 3 Dislocation.

Grade 3 Dislocation	λ (Stretch)	Total Force (N)	X-Moment (Nm)	Y-Moment (Nm)	Z-Moment (Nm)
Pectineus	2.009	2967.04	17.4055	20.1682	4.6945
Adductor Brevis	1.658	105.68	0.9486	0.8630	-0.0649
Adductor Longus	1.588	14.46	0.1479	0.0152	0.0052
Adductor Magnus Minimus	1.560	20.52	0.2135	-0.0082	0.0041
Adductor Magnus Middle	1.414	3.49	0.0359	-0.0083	-0.0026
Adductor Magnus Posterior	1.281	0.71	0.0068	-0.0071	-0.0011
Gracilis	1.417	0.77	0.0093	0.0032	-0.0020

5.2 Grade 4 Dislocation Results

For Grade 4, ossification center is above the level of the superolateral margin of the acetabulum. The femoral head was fully dislocated and positioned on the posterior wall of the acetabulum. Specifically, the center of the femoral head was placed at x = -10.05 mm, y = 12.69 mm, and z = 1.87 mm relative to the origin located at the center of the acetabulum. Table 5-2 provides the force and moment contribution of the adductor muscles under Pavlik Harness constraints. Although, Grade 4 was not initially reduced utilizing Pavlik harness constraints, the anatomical computational model enabled the use of external forces applied to the femoral head. It was found that depending on dislocation, forces as low as 10 N can be applied to free the femoral head and bring it back to the acetabulum as seen in Figure 5-3. These results will be discussed in detail in the last chapter. In addition, Figure 5-4 and Figure 5-5 exhibit a comparison between the forces developed by the adductors. It can be observed from these results that the Pectineus and the Adductor Brevis are the main contributors when the Pavlik harness is used.

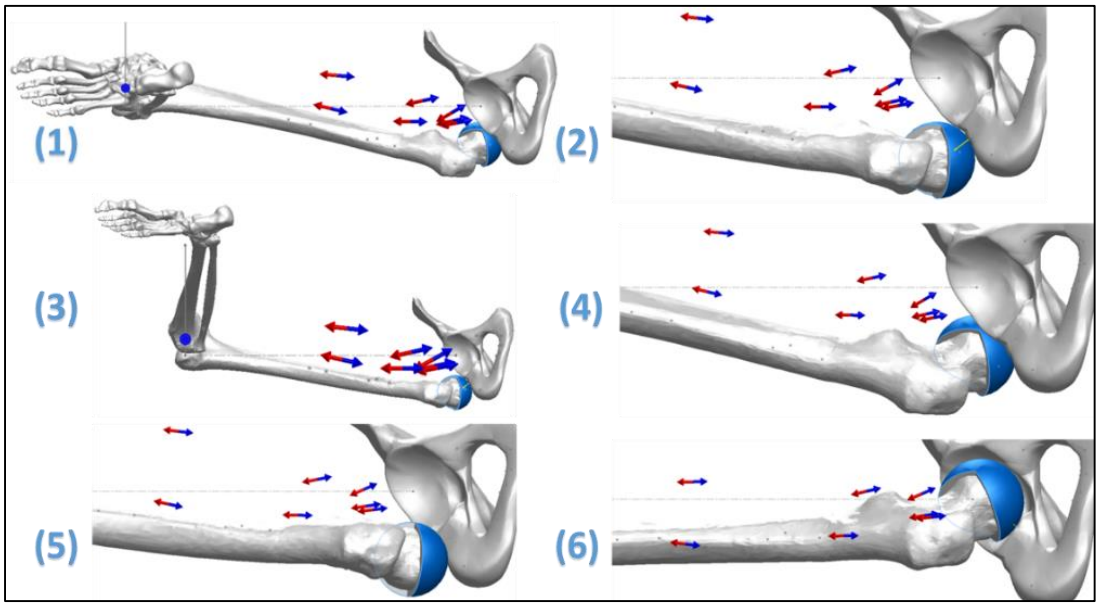

Figure 5-3: Grade 4 Dislocation on Ten-Week Old Female Infant (XZ Plane).

Table 5-2: Muscle Force and Moment Contribution on Grade 4 Dislocation.

Grade 4 Dislocation	λ (Stretch)	Total Force (N)	X-Moment (Nm)	Y-Moment (Nm)	Z-Moment (Nm)
Pectineus	2.153	2907.02	7.1963	12.1199	-0.3056
Adductor Brevis	1.729	79.65	0.4442	0.4848	-0.0833
Adductor Longus	1.667	11.78	0.0693	-0.0121	0.0175
Adductor Magnus Minimus	1.640	16.62	0.0974	-0.0394	0.0314
Adductor Magnus Middle	1.460	2.15	0.0162	-0.0075	0.0020
Adductor Magnus Posterior	1.299	0.39	0.0033	-0.0040	0.0001
Gracilis	1.432	0.42	0.0044	0.0014	-0.0009

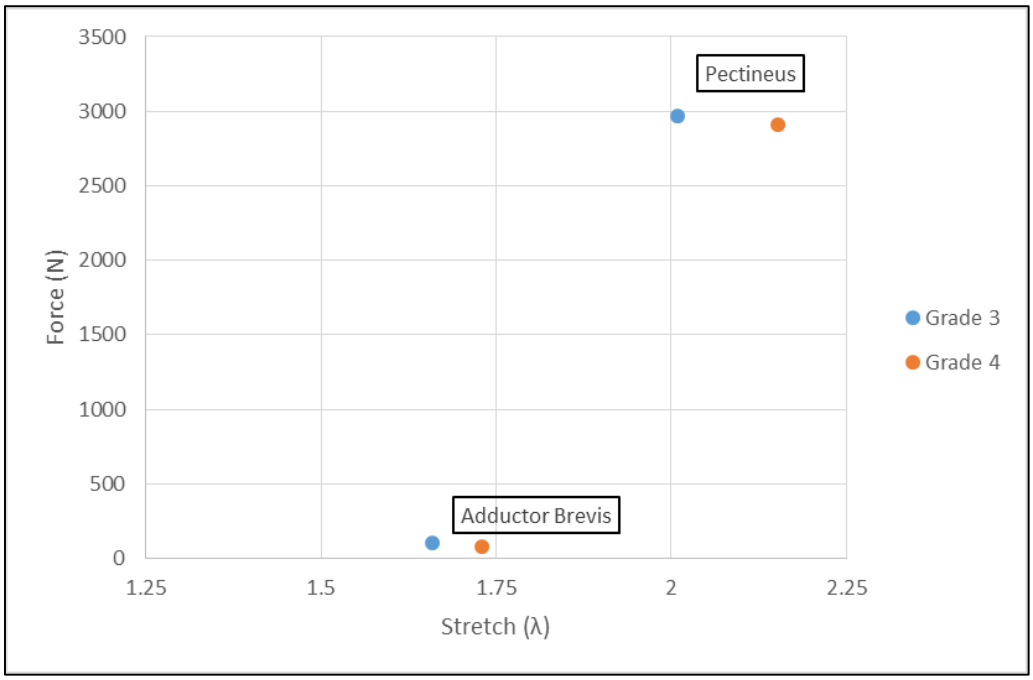

Figure 5-4: Muscle Force Contribution Comparison for Pectineus and Brevis.

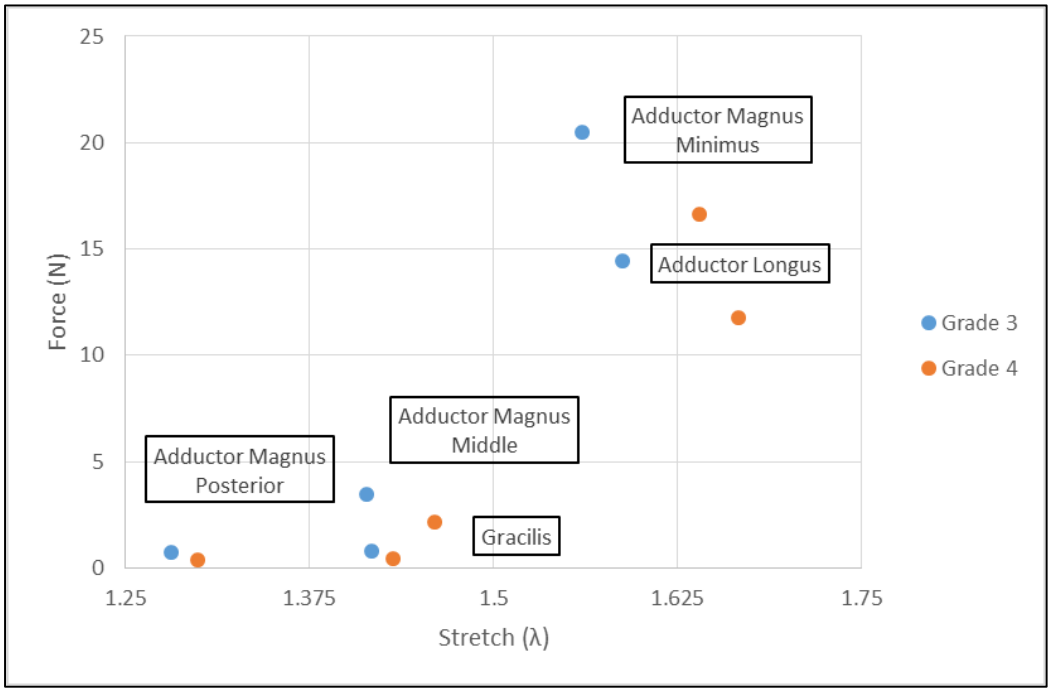

Figure 5-5: Muscle Force Contribution Comparison for Adductor Longus, Adductor Magnus and Gracilis.

CHAPTER 6: CONCLUSION

As expected, Grades 1 and 2 were successfully reduced. This is consistent with previous studies based on a synthetic model [51] as well as from clinical observation [40]. Grade 3 was successfully reduced while Grade 4 dislocation was not. However, Grade 4 dislocation reduction was achieved by an external rotation of the lower extremity followed by a semi-circular path taken by the femoral head along the posterior wall of the acetabulum along the ischial plane, and the subsequent entrance into the acetabulum via the acetabular notch as seen in Figure 6-1.

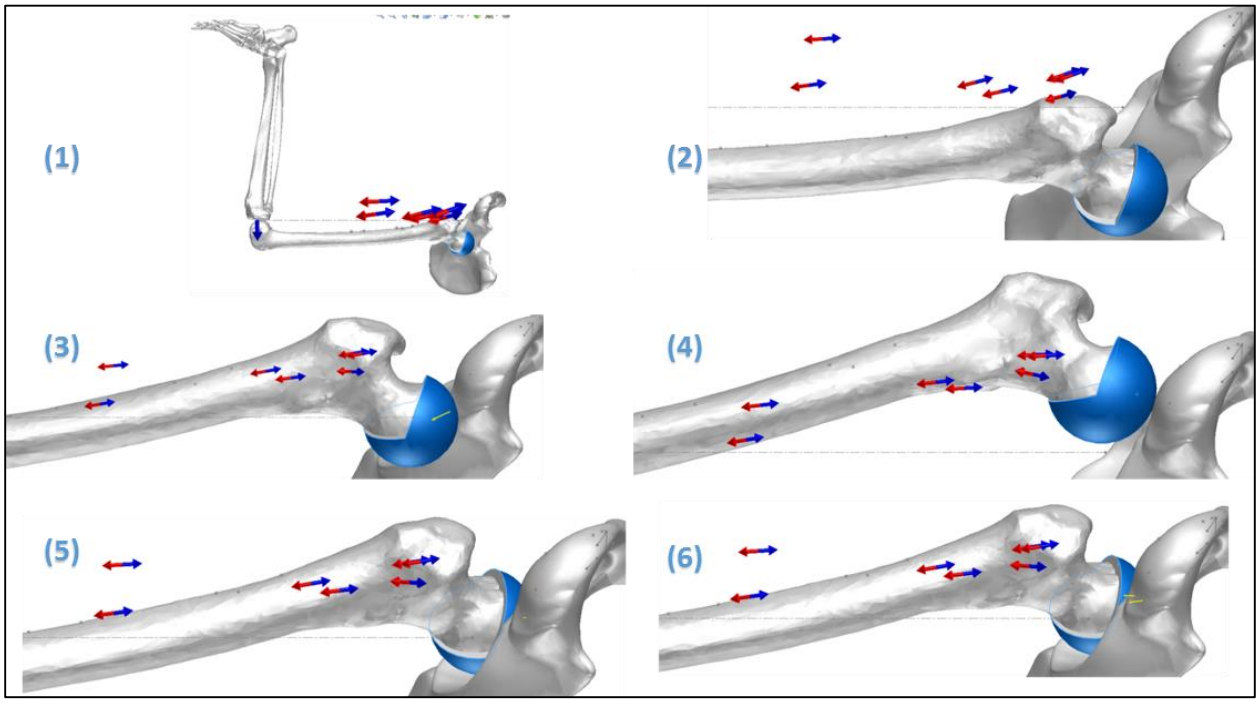

Figure 6-1: Grade 4 Dislocation on Ten-Week Old Female Infant (YZ Plane).

This path of reduction is generally consistent with Papadimitriou's clinical studies [38]. These studies indicate methods to accomplish reduction by avoiding the surgical release of adductor muscles. Papadimitriou's clinical results showed reduction occur in three sub-phases: (1)

the femoral head travels from the grade 4 dislocated position arriving at the ischial tuberosity, (2) the femoral head rides over the ischial tuberosity to the obturator foramen, and (3) the femoral head departs from the obturator foramen an enters the acetabulum via the acetabular notch, achieving reduction as explained in Figure 6-2. Moreover, Papadimitriou's studies showed successful reduction of severe dislocation by using this alternative hyperflexion procedure which uses the Hoffmann-Daimler harness keeping the hip flexed at 120°.

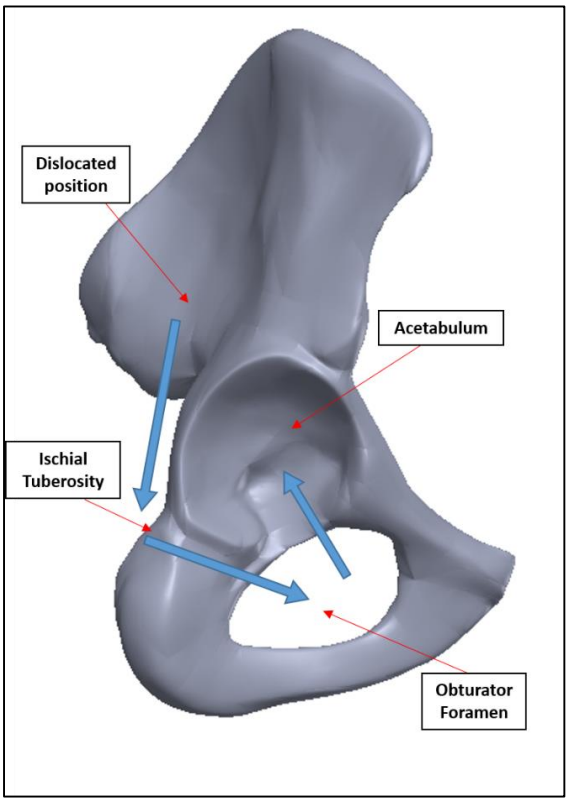

Figure 6-2: Reduction by Driving Femoral Head Posterior to the Acetabulum in an Inferior Direction.

In summary, a patient-derived geometry was successfully reconstructed to model the right lower extremity of a ten-week old female infant. The model developed on this dissertation allows

for the detailed study of the biomechanics of developmental dysplasia of the hip and its treatment with the Pavlik harness. Results suggest muscle force contributions on hip reduction are functions of the severity of hip dislocation. Additionally, findings strongly indicate muscle tensions contribute to reduction with the harness for subluxated and intermediate dislocations (Grades 1-3). It is also notable that the force contributions of the Pectineus and Adductor Brevis favor reduction significantly in Grades 1-3 while it disfavors reduction in Grade 4. The latter dislocations, which have been considered irreducible by most physicians, could be reduced by using a hyperflexion method. Further optimization of the Pavlik harness configuration may help improve the effectiveness of treatment of developmental dysplasia of the hip. This multi-physics computational approach is consistent with clinical observations reported in the literature and may potentially provide physicians means to determine modifications to evaluate treatment that could lead to new insights for non-surgical management of developmental dysplasia of the hip by passive reduction with the Pavlik harness or in combination with other orthosis.

In addition, the work developed on this dissertation leaves the door open to include some of the neglected assumptions to improve the lower limb computational model. For instance, the absence of the abductor muscles, which may influence total force and moment contribution can be included in the future. Moreover, the deformation of the non-ossified regions could be successfully quantified by implementing a finite element method. Lastly, it is important to mention that the functionality and design of the harness has not been modified in more than half a century. The force and moment quantification method developed on this dissertation will not only optimize its use but it will certainly lead to future development of a new harness based on patient-specific information.

APPENDIX: PUBLICATIONS, PRESENTATIONS AND AWARDS

Referred Journal Papers:

1. Huayamave, V., Rose, C., Divo, E., Moslehy, F., Kassab, A.J., Price, C., "*A Patient-Specific Model of the Biomechanics of Hip Reduction for Neonatal Developmental Dysplasia of the Hip: investigation of anteversion angle effects for low to severe grades of DDH*," Journal of Biomechanics, (in preparation 2015).
2. Huayamave, V., Rose, C., Serra, S., Jones, B., Divo, E., Moslehy, F., Kassab, A.J., Price, C., "*A Patient-Specific Model of the Biomechanics of Hip Reduction for Neonatal Developmental Dysplasia of the Hip: investigation of strategies for low to severe grades of DDH*," Journal of Biomechanics, (In press, DOI: 10.1016/j.jbiomech.2015.03.031).

Referred Conference Papers:

1. Huayamave, V., Rose, C., Zwawi, M., Divo, E., Moslehy, F., Kassab, A.J., Price, C., "*Mechanics of Hip Dysplasia Reduction in Infants with the Pavlik Harness using Patient Specific Geometry*," Proceedings of ASME-IMECE 2014, Montreal, Canada, November 14-20, 2014.

Poster Presentations:

1. Huayamave, V., Rose, C., Serra, S., Jones, B., Divo, E., Moslehy, F., Kassab, A.J., Price, C., "*Mechanics of Hip Dysplasia Reduction with the Pavlik Harness: Recent Developments for IHDI Grade 4 Dislocations*," CMBBE 2014, Amsterdam, The Netherlands, October 13-15, 2014.
2. Huayamave, V., Rose, C., Serra, S., Jones, B., Divo, E., Moslehy, F., Kassab, A.J., Price, C., "*Mechanics of Hip Dysplasia Reduction in Infants with the Pavlik Harness using Patient Specific Geometry*," WCB 2014, Boston, MA, July 6-11, 2014.

3. Huayamave, V., Divo, E., Kassab, A.J., "*An Optimization Approach for Hip Dysplasia using the Pavlik Harness*," SHPE 2011, Anaheim, CA, October 26-30, 2011.

Invited Talks:

1. Huayamave, V., "*Mechanics of Hip Dysplasia Reduction in Infants*," SHPE 2014, Detroit, MI, November 5- November 9, 2014.
2. Huayamave, V., and Rose, C., "*Mechanics of Hip Dysplasia Reduction in Infants with the Pavlik Harness using Patient Specific Geometry*," POSNA 2014, Hollywood, CA, April 30- May 3, 2014.

Awards:

1. McKnight Dissertation Fellowship, Florida Education Fund (FEF). 2014
2. ASME International Mechanical Engineering Congress and Exposition (IMECE). Technical Paper Competition Award. 2014.

LIST OF REFERENCES

1. Cohen, E.R., J. Feinglass, J.H. Barsuk, C. Barnard, A. O'Donnell, W.C. McGaghie, and D.B. Wayne, *Cost savings from reduced catheter-related bloodstream infection after simulation-based education for residents in a medical intensive care unit.* Simulation in healthcare, 2010. **5**(2): p. 98-102.
2. Gardner, R., T.B. Walzer, R. Simon, and D.B. Raemer, *Obstetric simulation as a risk control strategy: course design and evaluation.* Simulation in Healthcare, 2008. **3**(2): p. 119-127.
3. Bleck, E.E. and K.A.B. Michael, *Children's orthopaedics and fractures*. 2010: Springer Science & Business Media.
4. Benson, M., J. Fixsen, M. Macnicol, and K. Parsch, *Children's orthopaedics and fractures*. 2010: Springer.
5. Salter, R.B., *Etiology, pathogenesis and possible prevention of congenital dislocation of the hip.* Canadian Medical Association Journal, 1968. **98**(20): p. 933.
6. Dezateux, C. and K. Rosendahl, *Developmental dysplasia of the hip.* The Lancet, 2007. **369**(9572): p. 1541-1552.
7. Bialik, V., G.M. Bialik, S. Blazer, P. Sujov, F. Wiener, and M. Berant, *Developmental Dysplasia of the Hip: A New Approach to Incidence.* Pediatrics, 1999. **103**(1): p. 93-99.
8. Furnes, O., S.A. Lie, B. Espehaug, S.E. Vollset, L.B. Engesaeter, and L.I. Havelin, *Hip disease and the prognosis of total hip replacements: a review of 53 698 primary total hip replacements reported to the Norwegian Arthroplasty Register 1987-99.* Journal of Bone & Joint Surgery, British Volume, 2001. **83B**(4): p. 579-586.

9. Weinstein, S.L., S.J. Mubarak, and D.R. Wenger, *Developmental Hip Dysplasia and Dislocation Part II.* The Journal of Bone and Joint Surgery, 2003. **85**(10): p. 2024-2035.

10. Weinstein, S.L., *Natural history of congenital hip dislocation (CDH) and hip dysplasia.* Clinical orthopaedics and related research, 1987. **225**: p. 62-76.

11. Coleman, S.S., *Congenital dysplasia and dislocation of the hip*. 1978: Mosby.

12. Ortolani, M., *Congenital hip dysplasia in the light of early and very early diagnosis.* Clinical Orthopaedics And Related Research, 1976(119): p. 6-10.

13. Watanabe, R.S., *Embryology of the human hip.* Clinical orthopaedics and related research, 1974. **98**: p. 8-26.

14. Stanisavljevic, S., *Diagnosis and treatment of congenital hip pathology in the newborn*. 1964: Williams & Wilkins Co.

15. Wilkinson, J.A., *Prime factors in the etiology of congenital dislocation of the hip.* Journal of Bone & Joint Surgery, British Volume, 1963. **45**(2): p. 268-283.

16. Bjerkreim, I., *Congenital dislocation of the hip joint in Norway.* Acta Orthopaedica, 1974. **45**(S157): p. 1-88.

17. Wynne-Davies, R., *A family study of neonatal and late-diagnosis congenital dislocation of the hip.* Journal of medical genetics, 1970. **7**(4): p. 315.

18. Coleman, S.S., *Congenital dysplasia of the hip in the Navajo infant.* Clinical orthopaedics and related research, 1968. **56**: p. 179-194.

19. Dunn, P., *Perinatal observations on the etiology of congenital dislocation of the hip.* Clinical orthopaedics and related research, 1976. **119**: p. 11-22.

20. Dunn, P., *Congenital dislocation of the hip (CDH): necropsy studies at birth.* Proceedings of the Royal Society of Medicine, 1969. **62**(10): p. 1035.

21. Wynne-Davies, R., *Acetabular dysplasia and familial joint laxity: two etiological factors in congenital dislocation of the hip A review of 589 patients and their families.* Journal of Bone & Joint Surgery, British Volume, 1970. **52**(4): p. 704-716.

22. Chan, A., K.A. McCaul, P.J. Cundy, E.A. Haan, and R. Byron-Scott, *Perinatal risk factors for developmental dysplasia of the hip.* Archives of Disease in Childhood-Fetal and Neonatal Edition, 1997. **76**(2): p. F94-F100.

23. Ráliš, Z. and B. McKibbin, *Changes in shape of the human hip joint during its development and their relation to its stability.* Journal of Bone & Joint Surgery, British Volume, 1973. **55**(4): p. 780-785.

24. Skirving, A. and W. Scadden, *The African neonatal hip and its immunity from congenital dislocation.* Journal of Bone & Joint Surgery, British Volume, 1979. **61**(3): p. 339-341.

25. Blair, P.S., P. Sidebotham, C. Evason-Coombe, M. Edmonds, E.M. Heckstall-Smith, and P. Fleming, *Hazardous cosleeping environments and risk factors amenable to change: case-control study of SIDS in south west England.* Bmj, 2009. **339**: p. b3666.

26. Crawford, A.H., C.T. Mehlman, and R.W. Slovek, *The fate of untreated developmental dislocation of the hip: long-term follow-up of eleven patients.* Journal of Pediatric Orthopaedics, 1999. **19**(5): p. 641.

27. Barlow, T., *Early diagnosis and treatment of congenital dislocation of the hip.* Journal of Bone & Joint Surgery, British Volume, 1962. **44**(2): p. 292-301.

28. Bialik, V., J. Fishman, J. Katzir, and M. Zeltzer, *Clinical assessment of hip instability in the newborn by an orthopedic surgeon and a pediatrician.* Journal of Pediatric Orthopaedics, 1986. **6**(6): p. 703-705.

29. Tredwell, S.J. and H.M. Bell, *Efficacy of neonatal hip examination.* Journal of Pediatric Orthopaedics, 1981. **1**(1): p. 61-65.

30. USPSTF, *Screening for developmental dysplasia of the hip: recommendation statement.* Journal of the American Academy of Pediatrics, 2006. **117**(3): p. 898-902.

31. Ortolani, M., *La lussazione congenita dell'anca: nuovi criteri diagnostici e profilattico-correttivi*. 1948: Cappelli.

32. Aronsson, D.D., M.J. Goldberg, T.F. Kling, and D.R. Roy, *Developmental dysplasia of the hip.* Pediatrics, 1994. **94**(2): p. 201-208.

33. Graf, R., *New possibilities for the diagnosis of congenital hip joint dislocation by ultrasonography.* Journal of Pediatric Orthopaedics, 1983. **3**(3): p. 354-359.

34. Yousefzadeh, D. and J. Ramilo, *Normal hip in children: correlation of US with anatomic and cryomicrotome sections.* Radiology, 1987. **165**(3): p. 647-655.

35. Tönnis, D., *Congenital hip dislocation--avascular necrosis: necrosis of the femoral head as a complication of different conservative and operative methods of reduction in congenital dislocation of the hip: collective statistics* ed. D. Tönnis and G. Anders. 1982: Thieme-Stratton ; Stuttgart ; New York : Georg Thieme Verlag.

36. Narayanan, U., K. Mulpuri, W.N. Sankar, N. Clarke, H. Hosalkar, and C.T. Price, *Reliability of a New Radiographic Classification for Developmental Dysplasia of the Hip.* Journal of pediatric orthopedics, 2014.

37. Pavlik, A., *Die funktionelle Behandlungsmethode mittels Riemenbügel als Prinzip der konservativen Therapie bei angeborener Hüftgelenksverrenkung der Säuglinge.* Z Orthop, 1957. **89**: p. 341-352.

38. Papadimitriou, N.G., A. Papadimitriou, J.E. Christophorides, T.A. Beslikas, and P.K. Panagopoulos, *Late-Presenting Developmental Dysplasia of the Hip Treated with the Modified Hoffmann-Daimler Functional Method.* Journal of Bone and Joint Surgery, 2007. **89**(-): p. 1258-1268.

39. Von Rosen, S., *Diagnosis and treatment of congenital dislocation of the hip joint in the new-born.* Journal of Bone & Joint Surgery, British Volume, 1962. **44**(2): p. 284-291 %@ 2049-4394.

40. Uras, I., O.Y. Yavuz, M. Uygun, H. Yldrm, and M. Kömürcü, *The efficacy of semirigid hip orthosis in the delayed treatment of developmental dysplasia of the hip.* Journal of Pediatric Orthopaedics B, 2014. **23**(4): p. 339-342.

41. Malvitz, T.A. and S.L. Weinstein, *Closed reduction for congenital dysplasia of the hip. Functional and radiographic results after an average of thirty years.* The Journal of Bone & Joint Surgery, 1994. **76**(12): p. 1777-1792.

42. Ramsey, P.L., S. Lasser, and G.D. MacEwen, *Congenital dislocation of the hip. Use of the Pavlik harness in the child during the first six months of life.* The Journal of Bone and Joint Surgery, American volume, 1976. **58**(7): p. 1000-1004.

43. Graf, R., *Hip Sonography: Diagnosis and Management of Infant Hip Dysplasia*, ed. H.U. Helilman. 2006, New York: Springer.

44. Kitoh, H., M. Kawasumi, and N. Ishiguro, *Predictive Factors for Unsuccessful Treatment of Developmental Dysplasia of the Hip by the Pavlik Harness.* Journal of Pediatric Orthopaedics 2009. **29**(6): p. 552-557.

45. Mubarak, S., S. Garfin, R. Vance, B. McKinnon, and D. Sutherland, *Pitfalls in the use of the Pavlik harness for treatment of congenital dysplasia, subluxation, and dislocation of the hip.* The Journal Of Bone And Joint Surgery, American Volume, 1981. **63**(8): p. 1239-1248.

46. Viere, R.G., J.G. Birch, J.A. Herring, J.W. Roach, and C.E. Johnston, *Use of the Pavlik harness in congenital dislocation of the hip. An analysis of failures of treatment.* The Journal of Bone and Joint Surgery, 1990. **72**(2): p. 238-244.

47. Weinstein, S.L., S.J. Mubarak, and D.R. Wenger, *Developmental Hip Dysplasia and Dislocation Part I.* The Journal of Bone & Joint Surgery, 2003. **85**(9): p. 1824-1832.

48. Harding, M.G.B., H.T. Harcke, J.R. Bowen, J.T. Guille, and J. Glutting, *Management of Dislocated Hips with Pavlik Harness Treatment and Ultrasound Monitoring.* Journal of Pediatric Orthopaedics, 1997. **17**(2): p. 189-198.

49. Atalar, H., U. Sayli, O.Y. Yavuz, I. Uraş, and H. Dogruel, *Indicators of successful use of the Pavlik harness in infants with developmental dysplasia of the hip.* International Orthopaedics, 2007. **31**(2): p. 145-150.

50. Grill, F., H. Bensahel, J. Canadell, P. Dungl, T. Matasovic, and T. Vizkelety, *The Pavlik Harness in the Treatment of Congenital Dislocating Hip: Report on a Multicenter Study of the European Paediatric Orthopaedic Society.* Journal of Pediatric Orthopaedics, 1988. **8**(1): p. 1-8.

51. Ardila, O.J., E.A. Divo, F.A. Moslehy, G.T. Rab, A.J. Kassab, and C.T. Price, *Mechanics of hip dysplasia reductions in infants using the Pavlik harness: A physics-based computational model.* Journal of Biomechanics, 2013. **46**(9): p. 1501-1507.

52. Rombouts, J.-J. and A. Kaelin, *Inferior (obturator) dislocation of the hip in neonates. A complication of treatment by the Pavlik harness.* Journal of Bone and Joint Surgery, British Volume, 1992. **74**(5): p. 708-710.

53. Maquet, P., *Biomechanics of Hip Dysplasia.* Acta Orthopaedica Belgica, 1999. **65**(3): p. 302-314.

54. Arnold, A.S., S. Salinas, D.J. Asakawa, and S.L. Delp, *Accuracy of muscle moment arms estimated from MRI-based musculoskeletal models of the lower extremity.* Computer Aided Surgery, 2000. **5**(2): p. 108-119.

55. BOMBELLI, R., R.F. SANTORE, and R. POSS, *Mechanics of the Normal and Osteoarthritic Hip A New Perspective.* Clinical Orthopaedics and Related Research, 1984. **182**: p. 69-78.

56. Pauwels, F., *Biomechanics of the normal and diseased hip*. 1976: Springer Science & Business Media.

57. Murphy, S.B., S.R. Simon, P.K. Kijewski, R.H. Wilkinson, and N.T. Griscom, *Femoral anteversion.* The Journal of Bone & Joint Surgery, 1987. **69**(8): p. 1169-1176.

58. Cibulka, M.T., *Determination and significance of femoral neck anteversion.* Physical therapy, 2004. **84**(6): p. 550-558.

59. Fabry, G.U.Y., G.D. Macewen, and A.R. Shandsjr, *Torsion of the Femur A FOLLOW-UP STUDY IN NORMAL AND ABNORMAL C0NDITI0NS.* The Journal of Bone & Joint Surgery, 1973. **55**(8): p. 1726-1738.

60. Borelli, G.A., J. Bernoulli, N. Elinger, and C.J. a Jesu, *De motu animalium*. 1743: Apud Petrum Gosse.

61. Marieb, E.N. and K. Hoehn, *Human anatomy & physiology*. 2007: Pearson Education.

62. Shier, D., J. Butler, and R. Lewis, *Hole's Human Anatomy*. 1996: McGraw-Hill.

63. Alexander, R.M. and A. Vernon, *The dimensions of knee and ankle muscles and the forces they exert.* Journal of Human Movement Studies, 1975. **1**(1): p. 115-123.

64. Fukunaga, T., R. Roy, F. Shellock, J. Hodgson, M. Day, P. Lee, H. Kwong-Fu, and V. Edgerton, *Physiological cross-sectional area of human leg muscles based on magnetic resonance imaging.* Journal of Orthopaedic Research, 1992. **10**(6): p. 926-934.

65. Lieber, R.L., *Skeletal muscle structure, function, and plasticity*. 2009: Lippincott Williams & Wilkins Baltimore, MD:.

66. Zatsiorsky, V.M. and B.I. Prilutsky, *Biomechanics of skeletal muscles*. 2012, Champaign, IL: Human Kinetics.

67. Huijing, P.A., *Muscle as a collagen fiber reinforced composite: a review of force transmission in muscle and whole limb.* Journal of Biomechanics, 1999. **32**(4): p. 329-345.

68. Dostal, W.F. and J.G. Andrews, *A three-dimensional biomechanical model of hip musculature.* Journal of Biomechanics, 1981. **14**(11): p. 803-812.

69. Murray, W.M., T.S. Buchanan, and S.L. Delp, *Scaling of peak moment arms of elbow muscles with upper extremity bone dimensions.* Journal of biomechanics, 2002. **35**(1): p. 19-26.

70. Van Zuylen, E., A. Van Velzen, and J.D. van der Gon, *A biomechanical model for flexion torques of human arm muscles as a function of elbow angle.* Journal of Biomechanics, 1988. **21**(3): p. 183-190.

71. Jensen, R.H. and D.T. Davy, *An investigation of muscle lines of action about the hip: A centroid line approach vs the straight line approach.* Journal of Biomechanics, 1975. **8**(2): p. 103-110.

72. Jensen, R.H. and W.K. Metcalf, *A systematic approach to the quantitative description of musculo-skeletal geometry.* Journal Of Anatomy, 1975. **119**(Pt 2): p. 209-221.

73. Blemker, S.S. and S.L. Delp, *Three-dimensional representation of complex muscle architectures and geometries.* Annals of biomedical engineering, 2005. **33**(5): p. 661-673.

74. Gao, F., M. Damsgaard, J. Rasmussen, and S.T. Christensen, *Computational method for muscle-path representation in musculoskeletal models.* Biological Cybernetics, 2002. **87**(3): p. 199-210.

75. Tsuang, Y.H., G.J. Novak, O.D. Schipplein, A. Hafezi, J.H. Trafimow, and G.B.J. Andersson, *Trunk muscle geometry and centroid location when twisting.* Journal of Biomechanics, 1993. **26**(4–5): p. 537-546.

76. Gatti, C.J. and R.E. Hughes, *Optimization of muscle wrapping objects using simulated annealing.* Annals of biomedical engineering, 2009. **37**(7): p. 1342-1347.

77. Hill, A., *The heat of shortening and the dynamic constants of muscle.* Proceedings of the Royal Society of London B: Biological Sciences, 1938. **126**(843): p. 136-195.

78. Ebashi, S. and M. Endo, *Calcium and muscle contraction.* Progress in biophysics and molecular biology, 1968. **18**: p. 123-183.

79. Huxley, H., *The mechanism of muscular contraction.* Science, 1969. **164**(3886): p. 1356-1366.

80. Geeves, M.A. and K.C. Holmes, *Structural Mechanism of Muscle Contraction* Annual review of biochemistry, 1999. **68**(1): p. 687-728.

81. Winters, J.M., *Hill-based muscle models: a systems engineering perspective*, in *Multiple muscle systems*. 1990, Springer. p. 69-93.

82. Zajac, F.E., *Muscle and tendon: properties, models, scaling, and application to biomechanics and motor control.* Critical reviews in biomedical engineering, 1988. **17**(4): p. 359-411.

83. Chen, D.T. and D. Zeltzer, *Pump it up: Computer animation of a biomechanically based model of muscle using the finite element method*. Vol. 26. 1992: ACM.

84. Delp, S.L., *Surgery Simulation: A Computer Graphics System to Analyze and Design Musculoskeletal Reconstructions of the Lower Limb*, in *Department of Mechanical Engineering*. 1990, Stanford, California: Department of Mechanical Engineering.

85. Martins, J., E. Pires, R. Salvado, and P. Dinis, *A numerical model of passive and active behavior of skeletal muscles.* Computer methods in applied mechanics and engineering, 1998. **151**(3): p. 419-433.

86. Friden, J. and R.L. Lieber, *Structural and mechanical basis of exercise-induced muscle injury.* Medicine and science in sports and exercise, 1992. **24**(5): p. 521-530.

87. Hill, A., *The series elastic component of muscle.* Proceedings of the Royal Society of London. Series B-Biological Sciences, 1950. **137**(887): p. 273-280.

88. Fung, Y.-C., *Mathematical representation of the mechanical properties of the heart muscle.* Journal of biomechanics, 1970. **3**(4): p. 381-404.

89. Magid, A. and D. Law, *Myofibrils bear most of the resting tension in frog skeletal muscle.* Science, 1985. **230**(4731): p. 1280-1282.

90. Stecco, C., A. Porzionato, V. Macchi, C. Tiengo, A. Parenti, R. Aldegheri, V. Delmas, and R. De Caro, *A histological study of the deep fascia of the upper limb.* Italian Journal of Anatomy and Embryology, 2006. **111**(2): p. 105-110.

91. Gajdosik, R.L., *Passive extensibility of skeletal muscle: review of the literature with clinical implications.* Clinical biomechanics, 2001. **16**(2): p. 87-101.

92. Snyder, R.W., *Large deformation of isotropic biological tissue.* Journal of biomechanics, 1972. **5**(6): p. 601-606.

93. Fung, Y., *Elasticity of soft tissues in simple elongation.* American Journal of Physiology--Legacy Content, 1967. **213**(6): p. 1532-1544.

94. Rho, J.-Y., L. Kuhn-Spearing, and P. Zioupos, *Mechanical properties and the hierarchical structure of bone.* Medical engineering & physics, 1998. **20**(2): p. 92-102.

95. Snethen, K.G., *A Computed Tomography-Based Model of the Infant Hip Anatomy for Dynamic Finite Element Analysis of Hip Dysplasia Biomechanics*. 2013, University of Central Florida Orlando, Florida.

96. Delp, S.L., F.C. Anderson, A.S. Arnold, P. Loan, A. Habib, C.T. John, E. Guendelman, and D.G. Thelen, *OpenSim: open-source software to create and analyze dynamic simulations of movement.* Biomedical Engineering, IEEE Transactions on, 2007. **54**(11): p. 1940-1950.

97. Delp, S.L. and J.P. Loan, *A computational framework for simulating and analyzing human and animal movement.* Computing in Science & Engineering, 2000. **2**(5): p. 46-55.

98. Arnold, E.M., S.R. Ward, R.L. Lieber, and S.L. Delp, *A model of the lower limb for analysis of human movement.* Annals of Biomedical Engineering, 2010. **38**(2): p. 269-279.

99. Hensinger, R.N., *Standards in Pediatric Orthopedics*. 1986, New York: Raven Press.

100. NIH, *National Institute of Health and US National Library of Medicine, "The Visible Human Project,"* http://www.nlm.nih.gov/research/visible/visible_human.html. 2009.

101. Sankar, W.N., C.O. Neubuerger, and C.F. Moseley, *Femoral anteversion in developmental dysplasia of the hip.* Journal of Pediatric Orthopaedics, 2009. **29**(8): p. 885-888.

102. Delp, S.L., A.V. Komattu, and R.L. Wixson, *Superior displacement of the hip in total joint replacement: Effects of prosthetic neck length, neck-stem angle, and anteversion angle on the moment-generating capacity of the muscles.* Journal of Orthopaedic Research, 1994. **12**(6): p. 860-870.

103. Kelley, L.L. and C. Petersen, *Sectional anatomy for imaging professionals*. 2013: Elsevier Health Sciences.

104. CDC, *Centers for Disease and Prevention, "Birth to 24 months: Girls Length-for-age percentiles and Weight-for-age percentiles,"* http://www.cdc.gov/growthcharts/who_charts.htm 2009.

105. Drillis, R. and R. Contini, *Body Segment Parameters*. 1966, New York University School of Engineering and Science: New York.

106. Iwasaki, K., *Treatment of congenital dislocation of the hip by the Pavlik harness. Mechanism of reduction and usage.* The Journal of Bone and Joint Surgery, 1983. **65**(6): p. 760-7.

107. Suzuki, S., *Reduction of CDH by the Pavlik harness. Spontaneous reduction observed by ultrasound.* Journal of Bone and Joint Surgery, British Volume, 1994. **76-B**(3): p. 460-462.

108. Fukiage, K., N. Yamasaki, and S. Suzuki, *Visualization of developmental dysplasia of the hip in infants by using three-dimensional magnetic resonance imaging.* Journal of Pediatric Orthopaedics B, 2014. **23**(2): p. 107-111.

109. Hill, A.V., *Is Relaxation an Active Process?* Proceedings of the Royal Society of London. Series B, Biological Sciences, 1949. **136**: p. 420-435.

110. Hill, A.V., *First and last experiments in muscle mechanics*. 1970: University Press Cambridge.

111. Fung, Y.-C., *Stress-strain-history relations of soft tissues in simple elongation.* Biomechanics: its foundations and objectives, 1972. **7**(-): p. 181-208.

112. Thelen, D.G., *Adjustment of muscle mechanics model parameters to simulate dynamic contractions in older adults.* Journal of biomechanical engineering, 2003. **125**(1): p. 70-77.

113. Friederich, J.A. and R.A. Brand, *Muscle fiber architecture in the human lower limb.* Journal of Biomechanics, 1990. **23**(1): p. 91-95.

114. Cowin, S.C. and S.B. Doty, *Tissue mechanics*. 2007: Springer Science & Business Media.